Pergamon

Geochimica et Cosmochimica Acta, Vol. 68, No. 4, pp. 893–916, 2004

0016-7037/04 $30.00 + .00

doi:10.1016/S0016-7037(03)00486-1

Mechanisms of weathering of meteorites recovered from hot and cold deserts and the formation of phyllosilicates

MARTIN R. LEE[1,*] and PHILIP A. BLAND[2]

[1]Division of Earth Sciences, University of Glasgow, Lilybank Gardens, Glasgow, G12 8QQ, UK
[2]Department of Earth Science and Engineering, South Kensington Campus, Imperial College, London, SW7 2AZ, UK

(*Received September* 23, 2002; *accepted in revised form June* 23, 2003)

Abstract—Petrographic, mineralogical and chemical analysis of naturally weathered equilibrated ordinary chondrites collected from 'hot' deserts and Antarctica has revealed striking similarities and also pronounced differences in weathering between the two environments. Terrestrial weathering in all meteorites studied is dominated by oxidation and hydration of Fe,Ni metal, producing Fe-oxides and oxyhydroxides that have partially replaced the metal grains and have also occluded primary intergranular pores to form veins. Troilite weathers readily in 'hot' desert environments but undergoes very little alteration under Antarctic conditions. Most of the primary porosity of ordinary chondrites has been occluded by the time that ~15 to 25% of the initial Fe^0 and Fe^{2+} has been oxidised to Fe^{3+} in both environments. Results from modelling the volume changes upon alteration of primary minerals to a range of weathering products demonstrates that the primary porosity of most meteorites is sufficient to accommodate weathering products. Dilation of primary pores and brecciation, which has been observed in parts of some meteorites, will only occur if the meteorite is especially metal-rich, or has a low primary porosity. These weathering products are absent from recent falls but have formed in a fall after ~100 yr of museum storage.

Cl-bearing akaganéite and hibbingite are common weathering products in Antarctic finds but occur in abundance in only one 'hot' desert meteorite, Daraj 014. The majority of Fe-rich weathering products in meteorites from both environments contain low, but variable concentrations of Si, Mg and Ca. In most meteorites a proportion of these elements are inferred to be present as a very finely crystalline mineral with a ~1.0-nm lattice fringe spacing; where seen within intragranular fractures this mineral has a topotactic relationship with olivine and orthopyroxene. In the heavily-weathered Antarctic finds ALHA 78045 and 77002, Si is concentrated in cronstedtite, a Fe-rich phyllosilicate. An unidentified hydrous Si-Fe-Ni-Mg mineral or gel has also partially replaced taenite in ALHA 78045. In addition to Fe-rich weathering products, 'hot' desert meteorites contain sulphates, Ca-carbonate and silica, whereas such minerals are largely absent from Antarctic finds. The abundance of silicate weathering products in Antarctic meteorites is unexpected and indicates that olivine and pyroxene undergo significant chemical weathering in these environments. As preterrestrial cronstedtite is abundant in CM2 carbonaceous chondrites, the Antarctic environment may be a powerful analog for aqueous alteration in the asteroidal parent bodies of primitive meteorites. *Copyright © 2004 Elsevier Ltd*

1. INTRODUCTION

Many thousands of meteorites have been recovered from 'hot' and cold deserts and they include rare and scientifically valuable finds from Mars, the Moon and asteroidal parent bodies. Critical to the interpretation of mineralogical, chemical and isotopic data derived from these rocks is a detailed understanding of the mechanisms and rates of their interaction with terrestrial environments. Despite the aridity of 'hot' and cold deserts, chemical weathering of meteorites is rapid and Fe-oxide/oxyhydroxide and carbonate weathering products can form within a few tens of years (e.g., Jull et al., 1988; Bland et al., 1998a; Barrat et al., 1999). The most obvious effect of weathering is oxidation of Fe^0 and Fe^{2+} in reduced meteorites such as ordinary chondrites, producing a range of Fe-oxides and Fe-oxyhydroxides ('rust'). The progress of weathering reactions can be quantified by measuring the abundance of Fe^0-, Fe^{2+}- and Fe^{3+}-bearing minerals using Mössbauer spectroscopy (Bland et al., 1998a, 1998b) and also by reduction in intensity of thermoluminescence (Benoit and Sears, 1999). The mechanisms of interaction of meteorites with their terrestrial environment has also been investigated by a number of chemical and isotopic studies (e.g., Jull et al., 1988; Velbel et al., 1991; Ash and Pillinger, 1995; Stelzner and Hiede, 1996; Stelzner et al., 1999).

Despite the importance of terrestrial weathering in modifying the mineralogical, chemical and isotopic composition of meteorites, only one previous study has specifically addressed the potential formation of clay and phyllosilicate weathering products (Gooding, 1986). The possible presence of these minerals is however of particular importance because clays and phyllosilicates are among the best mineralogical indicators of preterrestrial aqueous alteration of meteorites within asteroidal and planetary regoliths (e.g., Barber, 1981, 1985). One of the main reasons why such minerals have not been previously identified in terrestrially weathered meteorites is because clays and phyllosilicates are difficult to characterise using chemical, isotopic or spectroscopic analysis of bulk samples, especially where present at low concentrations.

Here we report results of a study of meteorite terrestrial weathering products using high-resolution imaging and analysis techniques, principally scanning and transmission electron microscopy (SEM, TEM) and electron probe microanalysis

* Author to whom correspondence should be addressed (m.lee@earthsci.gla.ac.uk).

(EPMA). We analysed a suite of equilibrated ordinary chondrite (L5 and L6) finds from 'hot' deserts (Arizona [USA], Nullarbor [Australia] and Sahara [Algeria and Libya]) and Antarctica that have been previously spectroscopically and isotopically analysed (Bland et al., 1998a, 1998b; Bland et al., 2000a). In addition, we have studied two equilibrated ordinary chondrite falls to ensure that the minerals that we have interpreted as terrestrial weathering products do not form before the fall of the meteorite. The work reported here has focused on determining the mechanisms of weathering at micrometre- to nanometre-scales and the mineralogy and chemical composition of weathering products. Results have unexpectedly shown that silicate mineral weathering products are commonplace in finds, especially those from Antarctica. These silicates include cronstedtite, a Fe-rich phyllosilicate that also occurs in CM2 carbonaceous chondrites. One implication of this study is that there may be many similarities between the chemical microenvironments within meteorites on the Antarctic ice at the present day and the conditions within asteroidal parent bodies of carbonaceous chondrites ~4.4 Ga ago.

2. ANALYTICAL PROCEDURES

Samples of weathered meteorites were made into double polished thin sections and mounted using Crystalbond resin, following the technique of Barber (1981). The thin sections were prepared in oil in an attempt to preserve any evaporite minerals, although this technique does not always work. These samples were first studied by transmitted and reflected light microscopy, then using backscattered electrons (BSE) in a Cambridge Instruments S360 SEM operated at 20 kV. X-ray maps were acquired using an Oxford Instruments ISIS system attached to the SEM. Areas of interest identified by SEM were chemically analysed using a Cameca SX50 electron probe operated at 20 kV with a 15-nA beam current. The electron beam was defocused to 5 to 10 μm diameter to limit volatilisation from beam-sensitive minerals. Data were corrected using an on-line PAP procedure. The TEM samples were prepared by attaching a 3.05-mm copper washer to the surface of the thin section with an epoxy resin, with the central ~0.5-mm-diameter hole positioned over an area of interest. Following extraction from the thin sections, the foils were thinned to electron-transparency using a Gatan DuoMill operated at 6 kV. The TEM samples were studied using a Philips Biotwin operated at 120 kV and a JEOL 200FX operated at 200 kV.

3. METEORITES STUDIED

We studied L5 and L6 ordinary chondrite finds from three 'hot' deserts (Table 1) and the Allan Hills area of Antarctica (Table 2) and two L6 falls (Table 1). Tables 1 and 2 include data on the terrestrial ages of the meteorites and the relative amounts of Fe^0 and Fe^{2+} that have been oxidised to Fe^{3+} (measured by Mössbauer spectroscopy), which is taken here to be directly proportional to the degree of terrestrial weathering of the meteorites. For comparison, the visual weathering classification of the meteorites, where available, is also listed. Earlier results from three of the meteorites analysed for this research programme (Forrest 009, ALHA 78045 and ALHA 77002) have been published elsewhere (Bland et al., 2000b; Lee and Bland, 2003; Lee et al., 2003). Note that the terrestrial weathering of ALHA 77002 has been previously studied by Ikeda and Kojima (1991), who concluded that its visual weathering grade (B) was too low for the amount of terrestrial alteration that they had identified. From an analysis of natural thermoluminescence, Benoit and Sears (1999) have suggested that ALHA 77002 had been exposed at the surface for $< 310 \times 10^3$ yr.

In this paper we make the following assumptions about the preterrestrial mineralogical and chemical composition of L5 and L6 ordinary chondrites. Firstly, they contained negligible quantities of Cl, Fe^{3+} and H_2O and so all of the Cl-, Fe^{3+}- and H_2O-bearing minerals now observed can be confidently ascribed to terrestrial weathering. This is supported by petrographic and Mössbauer spectroscopy results from L6 falls (see below). It is important to note that oxidation of iron can occur in asteroidal environments, but not within the parent body or bodies of L5/6 ordinary chondrites. We also assume that before they fell to Earth these meteorites contained no clays, phyllosilicates or evaporites. Smectite and carbonates have been described from unequilibrated ordinary chondrites including Semarkona (Hutchison et al., 1987) but not, to the authors' knowledge, from equilibrated ordinary chondrites. In addition, some halite and sylvite have been found in the H-chondrites Monahans (fell in 1998) and Zag (Rubin et al., 2002), but given the solubility of such minerals at the Earth's surface they are unlikely to survive prolonged terrestrial weathering. The average mineralogy of L class ordinary chondrites is taken from normative mineralogy data in McSween et al. (1991): olivine 44.83%, orthopyroxene 24.15%, total feldspar (albite + anothorthite + orthoclase) 10.3%, Fe,Ni metal 8.39%, troilite 5.8%, clinopyroxene 4.97%, chromite 0.78%, apatite 0.54% and ilmenite 0.24%.

The porosities of ordinary chondrites has been recently studied by Corrigan et al. (1997), Consolmagno and Britt (1998), Consolmagno et al. (1998), and Flynn et al. (1999). Results of these studies differ, possibly reflecting a significant variability inherent in ordinary chondrites. Corrigan et al. (1997) reported porosities from three L5/L6 falls of 2.6, 16.7 and 18.2%. These data are generally higher than the porosities of the L5/L6 falls studied by Flynn et al. (1999) of 4 ± 4, 10 ± 2, 11 ± 2 and 17 ± 1%. Consolmagno and Britt (1998) measured the porosities of seven L5 and L6 ordinary chondrites in the Vatican collection and found values of 0 ± 2.2, 2 ± 1.7, 5 ± 1.7, 6 ± 1.6, 7 ± 1.3, 9 ± 1.1 and 9 ± 2.6%. The mean of the 14 values above is 8.4%. Histograms of measured L chondrite porosities in Consolmagno et al. (1998, Fig. 4) shows that falls range from ~0 to 20%, with ~50% having ≤ 5% porosity, whereas non-Antarctic finds range from 0 to 10%, with ~80% having ≤ 5% porosity. By contrast, the measured porosity of Antarctic L chondrites ranges from 0 to 20% and is fairly evenly distributed over that range although the largest proportion (54%) have porosities of ~7.5 to 12.5%.

4. RESULTS

4.1. Weathering Products in Falls

We studied thin sections of two L6 falls, New Concord (fell 1860) and Barwell (fell 1965), both supplied by the British Museum of Natural History, to confirm that when they fall to

Table 1. Petrographic and mineralogical characteristics of the falls and hot desert finds used in this study.

Meteorite, class, Mass (Location of fall/find)	Terrestrial age (Oxidation)[8] (Weathering class)	Petrography of Fe, Ni and troilite	Extent of occlusion of primary porosity	Evidence for silicate dissolution?	Other comments
Barwell, L6, 44 kg[1] (Fall, England)	0.04 ka (0%) (n.a)	No alteration	None	No	
New Concord, L6, ~227 kg[1] (Fall, Ohio USA)	0.14 ka (n.d) (n.a)	Partial alteration of Fe, Ni grains (rims = ~15 μm).	Partial occlusion by Fe-sulphide (?pyrrhotite).	No	
Acfer 263, L6, 438 g[2] (Find, Algeria)	3.7 ± 1.3 ka[8] (2.8%) (n.d)	Partial alteration of Fe, Ni grains (rims = 6–9 μm).	Only in immediate vicinity of metal grains.	No	
Holbrook, L6, Not known[3] (Find, Arizona)	0.06 ka[8] (9.7%) (n.d)	Data not available	Mostly	No	Significant localised brecciation.
Daraj 014, L6, 395 g[4] (Find, Libya)	6.6 ± 1.3 ka[8] (14.9 %) (n.d)	Partial alteration of Fe, Ni grains (rims = 7–11 μm) and troilite. Some Fe, Ni grains more heavily altered.	Complete	No	
Billygoat Donga, L6, Not known (Find, Nullarbor)	7.7 ± 1.3 ka[8] (23.5 %) (n.d)	Fe,Ni and troilite heavily altered. Fe,Ni grains have thick laminated rims.	Complete	Very minor	Very finely crystalline weathering products with ~1.0-nm lattice fringe spacing.
Acfer 019, L6, 581 g[5] (Find, Algeria)	19.8 ± 1.3 ka[8] (31.8%) (n.d)	Fe,Ni metal heavily altered in parts. Some replacement of troilite.	Complete	Yes	Jarosite, Ca-carbonate, silica and Fe-silicate. Some brecciation.
Acfer 298, L6, 2 kg[6] (Find, Algeria)	42.4 ka[8,9] (35.1 %) (W4–5)	Little Fe,Ni metal or troilite remaining.	Complete	Yes	Gypsum, barite and jarosite. Some brecciation.
Forrest 009, L6, 1 kg[7] (Find, Nullarbor)	5.9 ± 1.3 ka[8] (38.4 %) (n.d)	Almost all Fe,Ni metal altered, but considerable volumes of troilite remain.	Complete	Yes	Porous silica pseudomorphs of silicate grains. Ca-carbonateveins. Desert varnish on outer surface[10]

[1] Total mass of shower, [2] Wlotzka (1993a), [3] This sample of the 1912 Holbrook shower was recovered in 1968, [4] Graham (1989), [5] Wlotzka (1990), [6] Wlotzka (1993b), [7] Graham(1990), [8] Bland et al. (1998b), [9] Age error not stated, [10] Lee and Bland (2003). n.a. denotes not applicable as the meteorite is a fall. n.d. denotes not determined.

Earth L6 meteorites are free of minerals that we interpret as weathering products. In an analysis of Barwell by Mössbauer spectroscopy, Bland et al. (1998b) were unable to detect any magnetic or paramegnetic Fe^{3+}, indicating that it is completely unweathered. These results agree very well with SEM results which showed that Fe,Ni and troilite grains are unaltered and intergranular pores are free of alteration products. By contrast, New Concord has significant evidence for alteration. Many of the Fe,Ni grains have a laminated rim of Fe- and O-rich alteration products (Fig. 1) and much of the intergranular porosity is filled by Fe-sulphides (probably pyrrhotite). Two generations of alteration products can clearly be distinguished in the SEM images (Fig. 1). The inner layer is discontinuous, a few micrometres thick and the alteration products have a relatively low Fe/O ratio. The outer layer is thicker, more continuous and the alteration products have a greater Fe/O ratio (Fig. 1c). Note that the outer layer alteration products contain measurable concentrations of Si (Fig. 1c). The thin section of New Concord was prepared in 1965 or 1966 (S. Russell, personal communication, 2003) and so assuming that no weathering has taken place after the rock slice was mounted on the glass slide and set in resin, alteration products in the New Concord sample represent 105 yr of 'museum weathering'.

4.2. Hot Desert Finds

4.2.1. Petrography of Fe-Rich Weathering Products

Results of the petrographic study of 'hot' desert finds are summarised in Table 1. These meteorites have mainly weathered by the alteration of Fe,Ni metal and troilite to hydrous Fe-rich minerals. Hereafter we refer to these weathering products as Fe-oxide/oxyhydroxides, a term that includes a range of minerals that cannot be readily distinguished from one another using SEM images or EPMA data. In early stages of weathering the Fe-oxide/oxyhydroxides form a rim to the Fe,Ni metal grains. This rim is initially narrow (few tens of micrometres) and discontinuous but becomes thicker, continuous and usually concentrically laminated with progressive weathering (Fig. 2). After oxidation of ~30% of the Fe^0 and Fe^{2+} in the bulk meteorite to Fe^{3+} most of the Fe,Ni metal has been completely replaced (Table 1). Troilite weathers at approximately the same rate as Fe,Ni metal, or slightly slower, but instead of forming a rim, the weathering products replace grain interiors leaving irregular or rectilinear volumes of troilite enclosed by Fe-oxide/oxyhydroxides (Fig. 3a). As troilite lacks a cleavage, these lineations may lie parallel to a {0001} parting. In addition to replacing metal and troilite grains, Fe-oxide/oxyhydroxide

Table 2. Petrographic and mineralogical characteristics of the Antarctic meteorites used in this study.

Meteorite, class[1] (Part sampled)[2] Mass[1]	Terrestrial age (Oxidation) (Weathering class)[1]	Petrography of Fe,Ni and troilite	Extent of occlusion of primary porosity	Evidence for silicate dissolution?	Other comments
ALHA 77001, L6 (Int. and ext.) 252 g	60 ± 60 ka[3] (3.1%)[6] (B)	Partial alteration of Fe,Ni grains (rims = 4–16 μm).	None	No	
ALHA 77180, L6 (Int. and ext.) 190.8 g	80 ± 70 ka[4] (4.1%)[7] (C)	Partial alteration of Fe,Ni grains (rims = 4–20 μm).	In immediate vicinity of Fe,Ni metal grains.	No	
ALHA 78104, L6 (Int. and ext.) 672.4 g	70 ± 70 ka[4] (5.3%)[6] (B)	Partial alteration of Fe,Ni grains (rims = 5–38 μm).	Extensive in patches.	No	
ALHA 78112, L6 (Int. and ext.) 2485 g	230 ± 70 ka[5] (13.6%)[6] (B)	Partial alteration of Fe,Ni grains (rims = 8–33 μm). Total replacement of Fe,Ni in external sample.	Complete apart for widest pores.	No	Some brecciation
ALHA 78045, L6 (Int.) 396.5 g	740 ± 80 ka[4] (23.3%)[6] (B/C)	Partial alteration of Fe,Ni grains (rims = 4–18 μm).	Complete	No	Some brecciation. Fe-silicate, Fe-Ni-Mg silicate, very finely crystalline ~1.0-nmmineral and Ca-carbonate.
ALHA 77002, L5 (Int.) 235.2 g	820 ± 80 ka[4] (31.5%)[6] (B)	Nearly complete alteration of Fe,Ni grains.	Complete	No	Extensive breccation. Fe-silicate and very finely crystalline ~1.0-nm mineral.

[1] Grossman (1994), [2] Int. denotes internal sample, ext. denotes external sample, [3] Nishiizumi et al. (1981), [4] Nishiizumi et al. (1989), [5] Nishiizumi et al. (1983), [6] Bland et al. (2000), [7] Bland, unpublished work.

weathering products occlude inter and intragranular pores, eventually producing interconnected networks of veins that are up to a few tens of micrometres in width (Figs. 3a and 3b). After ~15% of the original Fe^0 and Fe^{2+} has been oxidised, most of the intergranular porosity has been occluded (Table 1). In parts of Holbrook, Acfer 019 and Acfer 298, angular pieces of olivine, pyroxene and feldspar grains lie supported within weathering products (Fig. 3b), indicating that this brecciation took place during weathering. The other noticeable effect of weathering is dissolution of olivine and pyroxene, which can be recognised after ~23% oxidation (Table 1). The result of dissolution is to produce angular pores, often in a 'boxwork' structure (Fig. 3c) and these effects are most noticeable in the immediate vicinity of heavily weathered Fe,Ni metal and troilite grains (Fig. 3a). TEM images confirm that dissolution occurs in the immediate vicinity of Fe-oxide/oxyhydroxides and show that dissolution is directed along dislocations in olivine and pyroxene (Fig. 3d).

4.2.2. Chemical Composition of Fe-Rich Weathering Products

EPMA work has concentrated on weathering products within and surrounding Fe,Ni and troilite grains because most of the intra and intergranular veins are too narrow to yield analyses free of potential contamination from enclosing silicates. The weathering products are dominated by Fe, Ni, Si, Cl and S and all give low analytical totals. This indicates that the weathering products have a hydrous composition, but inter or intragranular porosity may also contribute to the low totals (Table 3).

Hot desert weathering products have an average of 75.9 wt.% Fe_2O_3 and 4.6 wt.% NiO (Table 3) and high Fe/Ni ratios (Fig. 4). Analyses of Fe,Ni metal grains and their corresponding weathering rims shows that rims on taenite grains (Fe/Ni = ~2.5) are composed of Fe-oxide/oxyhydroxides with Fe/Ni ratios mostly > 10 (corresponding to ~4–16 wt.% NiO). However, weathering products surrounding kamacite grains (Fe/Ni ~14–16) have Fe/Ni ratios of ~11 to 20 (corresponding to ~3–6 wt.% NiO) (Fig. 2). Note from Figure 4 that some weathering products from Daraj 014 have Fe/Ni ratios comparable to that of taenite, although they have formed by alteration of a grain of kamacite. Sulphur is present in low concentrations in all weathering products (Table 3) and even those within troilite grains have < 0.3 wt.% SO_2 (Table 3), demonstrating almost complete loss of that element from troilite during weathering.

The ternary diagram in Figure 4 shows that the Fe-rich weathering products in most meteorites have low concentrations of Cl (mean 1 wt.%, maximum 3 wt.%, Table 3). However, a number of analyses of a Fe,Ni metal rim from Daraj 014 had 12–20 wt.% Cl, with an average of 15.9 wt.% (Table 3). An EPMA traverse through the thick laminated rim on a different kamacite grain from the same meteorite revealed very high Cl concentrations whose average and maximum values were 4.5 and 21.5 wt.% respectively (Fig. 2). Cl does not correlate well with any of the other elements measured, including Fe. Importantly, the traverse in Figure 2 shows that Cl concentrations are lower at the margins of the laminated rim than in its interior and the greatest concentrations occur close to the remaining Fe,Ni

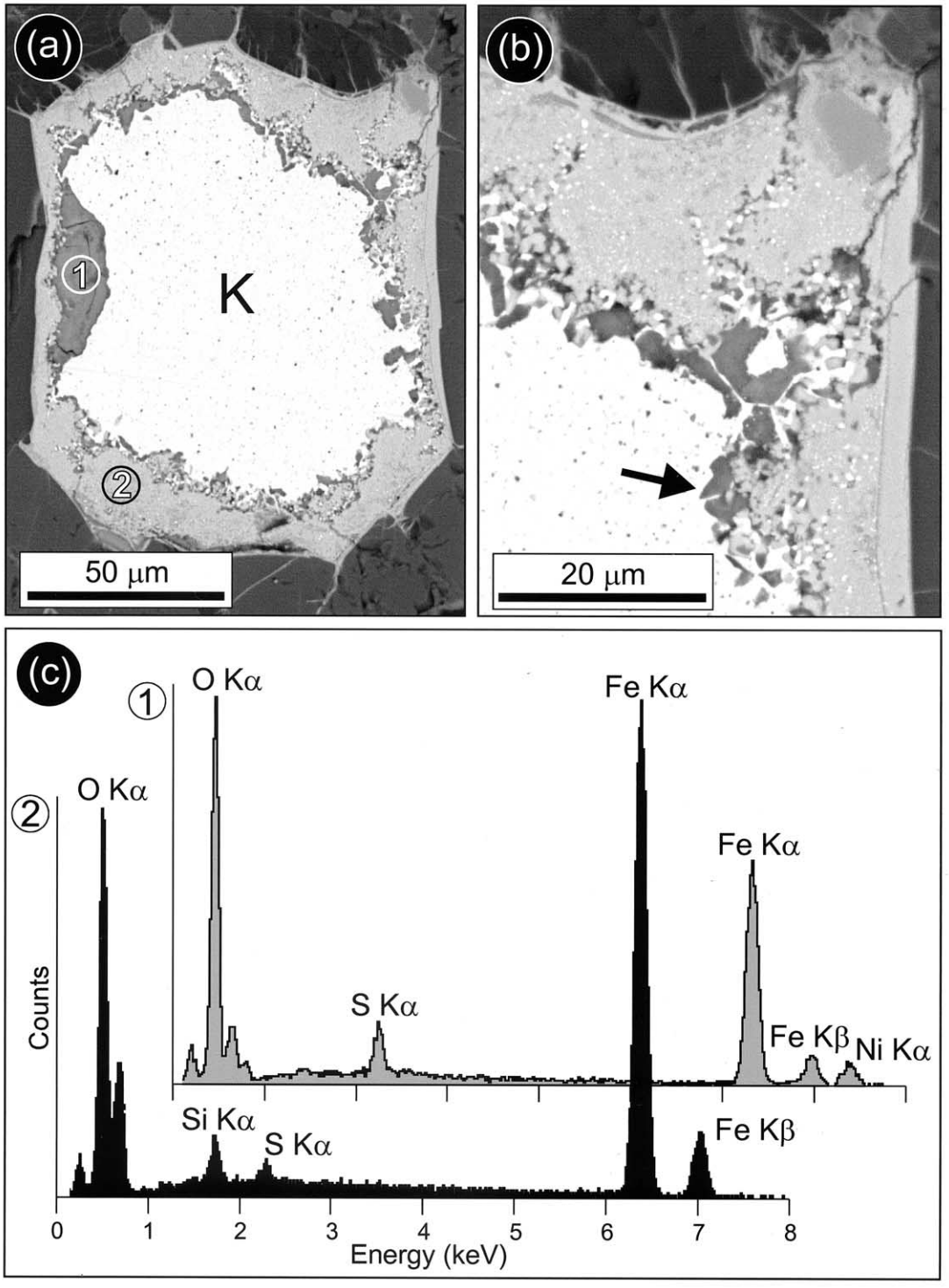

Fig. 1. Images and analyses of alteration products in New Concord. (a) BSE image of a Fe,Ni metal (kamacite) grain (white, K) surrounded by silicate minerals (dark grey). The kamacite grain is rimmed by two generations of alteration products. The inner layer (labelled 1), which is discontinuous, is composed of one or minerals with a relatively low mean atomic number whereas the outer layer (labelled 2) is continuous and is composed of one or minerals with a greater mean atomic number. Some of these alteration products have occluded pores and fractures in surrounding silicates to form veins. (b) BSE image of the upper right hand corner of the altered kamacite grain in (a). This image shows that the innermost alteration products have euhedral terminations where against the kamacite (arrowed) and the outer alteration products are speckled with submicrometre sized inclusions of kamacite. (c) X-ray spectra of the two generations of alteration products, taken from points 1 and 2 in (a). These spectra show that the two generations differ in Fe/O ratios and in concentrations of Si, S and Ni.

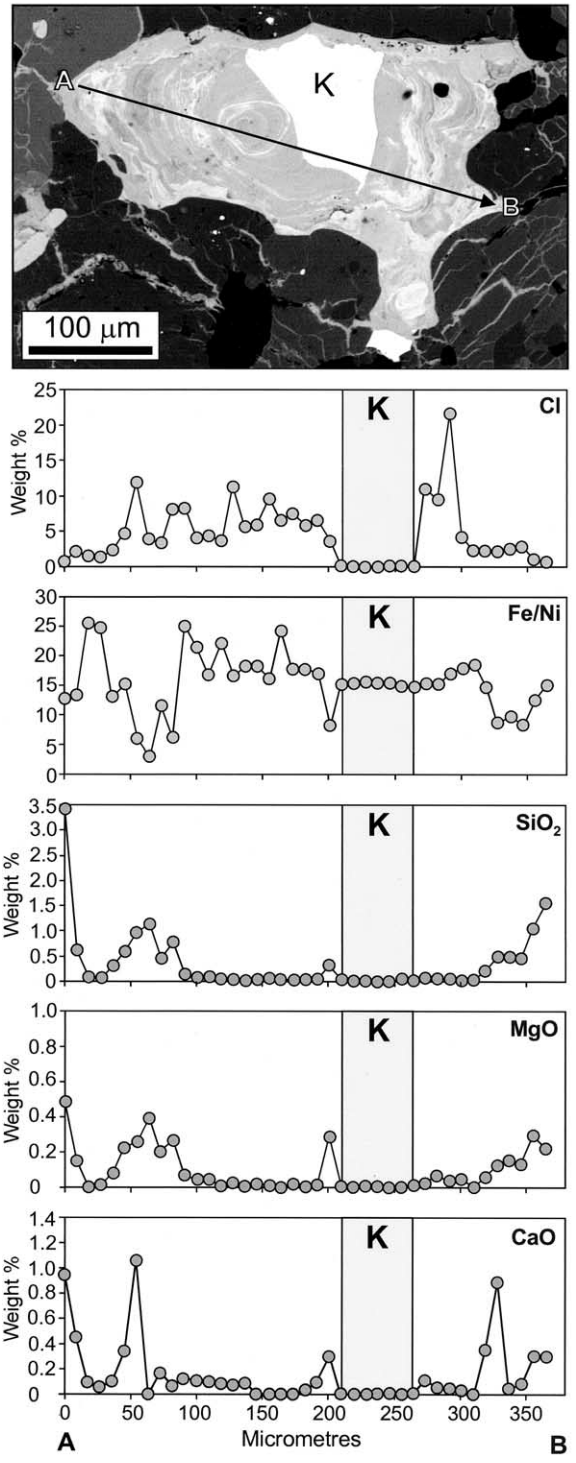

Fig. 2. BSE image of a weathered Fe, Ni metal (kamacite) grain from Daraj 014 and graphs with EPMA data from a 370-μm traverse across the grain from A to B. The BSE image shows that the kamacite grain (K) has been altered from the outside inwards, producing a thick concentrically laminated rim of weathering products (light grey) which also form veins within surrounding silicates. The graphs below show that Cl concentrations are lowest at the margins of the weathered grain and maximum values occur close to remaining kamacite (indicated by shaded area, labelled K, on the graphs). Fe/Ni ratios of the weathering products show a considerable range but SiO_2, MgO and CaO concentrations are all greatest at the margins of the altered grain.

metal. Data from this traverse are also plotted in the ternary diagram on Figure 4.

Fe-rich weathering products in 'hot' desert meteorites have an average of 3.5 wt.% SiO_2, 0.3 wt.% MgO and 0.4 wt.% Ca; note that Al is present in very low concentrations in all analyses (Table 3). Fe/Si ratios are high and analyses with the lowest Fe/Si ratios have greatest Mg concentrations (Fig. 5). The EPMA traverse from Daraj 014 (Fig. 2) shows a strong covariance between SiO_2, MgO and CaO with all three elements enriched in the outermost ~50 μm of the rim. One heavily weathered troilite grain in Acfer 019 contained discrete rectilinear volumes of weathering products a few tens of micrometres in size (Figs. 6a and 6b) with up to 14.7 wt.% SiO_2 (Table 3, Fig. 6). These Si-rich volumes are enclosed by weathering products with chemical compositions more typical of Fe-oxide/oxyhydroxides (Table 3).

4.2.3. Other Weathering Products

Other minerals that have formed by chemical weathering of 'hot' desert meteorites include jarosite (possibly hydronium jarosite), Ca-carbonate, Ca-sulphate, silica and barite (Table 1). Jarosite is intergrown with Fe-oxide/oxyhydroxides within pseudomorphs of primary grains, probably troilite, and has also partially occluded intergranular veins. Acfer 019 and Forrest 009 contain veins of Ca-carbonate up to 50 μm in width that cross-cut all objects, including volumes of Fe-oxide/oxyhydroxides (Fig. 6b). Ca-carbonate in Acfer 019 is compositionally relatively pure, containing an average of 98.6 wt.% $CaCO_3$, 0.4 wt.% $MgCO_3$, 0.9 wt.% $FeCO_3$ and 0.1 wt.% $MnCO_3$ (n = 11 analyses). One large vein in Acfer 019 has a lower layer composed of silica and an upper layer cemented by Ca-carbonate crystals that present euhedral crystal faces into open pores (Fig. 6c). EPMA data show that the silica is relatively pure SiO_2 and has low analytical totals, indicating a hydrous composition (Table 3). Silica was also found in Forrest 009 within a meshwork of alteration products that had formed by dissolution of olivine and pyroxene grains (Fig. 3c). Barite and Ca-sulphate, which are both uncommon in 'hot' deserts finds, occur in association with veins that have been partially occluded by Fe-oxide/oxyhydroxides. In the case of barite at least, its petrographic relationship indicates that it formed after the Fe-oxide/oxyhydroxides (Fig. 6d).

4.2.4. TEM Observations of Weathering Products

Ion thinned foils of all of the 'hot' desert finds apart from Holbrook were studied by TEM, although only Billygoat Donga was characterised by high-resolution imaging. Differential thinning between olivine, pyroxene and weathering products meant that studying the vein-filling minerals by TEM was challenging. However, high-resolution images of the interior of olivine and orthopyroxene grains from Billygoat Donga show that very small crystallites (approximately a few nanometres in size) of a mineral with a ~1.0-nm lattice fringe spacing are abundant weathering product within intragranular fractures. Within intergranular pores the crystallites are larger (~10–30 nm in length by ~3–10 nm thickness) and curved, forming subcircular structures (Fig. 7). The possible identity of this mineral is discussed in later sections.

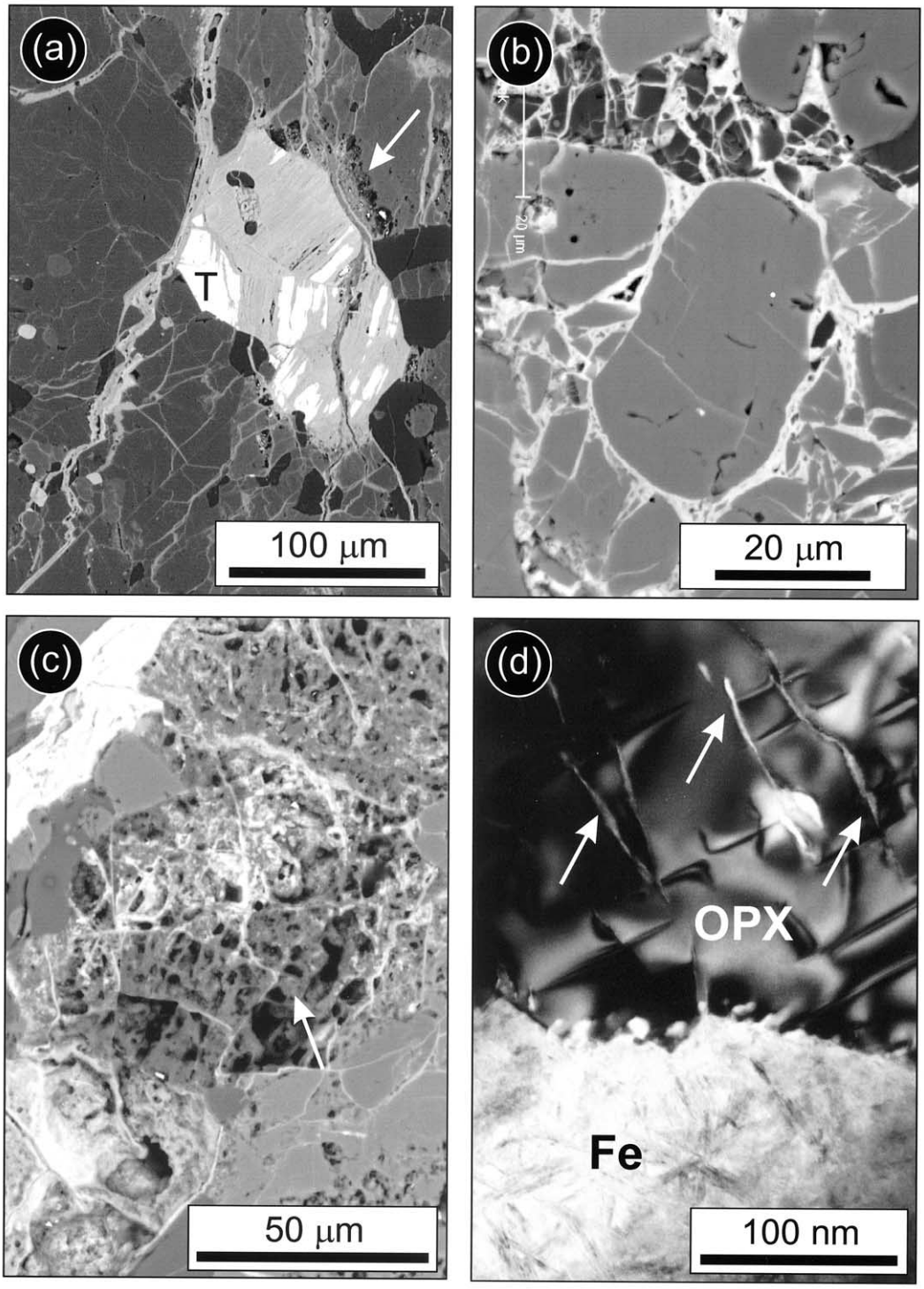

Fig. 3. Images of the weathered interiors of meteorites recovered from 'hot' deserts. (a) BSE image of a weathered troilite grain surrounded by olivine and orthopyroxene from Billygoat Donga. Only small rectilinear volumes of troilite (T, white) remain within the grain and are surrounded by Fe-oxide/oxyhydroxides (light grey). Veins of these weathering products also radiate outwards from the troilite grain. Some porosity remains in the centre of these veins and pores have also been produced by dissolution of silicates on the right hand side of the troilite grain (arrowed). (b) BSE image of an area of brecciation within Holbrook. Although some of the olivine, orthopyroxene and feldspar grains may just be heavily veined, rotation of some fragments has taken place (lower right hand side of the image). (c) BSE image of an area of olivine in Forrest 009 that has been partially dissolved, producing a 'boxwork' structure. The dark grey material within the boxwork (arrowed) is almost solely composed of Si and O. (d) Bright-field TEM image of the interface between a volume of finely crystalline Fe-oxide/oxyhydroxide (Fe) and orthopyroxene (OPX) in Acfer 298. The OPX contains narrow sinuous pores (arrowed) that have formed by selective dissolution of strained crystal structure surrounding dislocations.

Table 3. Chemical composition of Fe-rich weathering products determined by EPMA.

	All hot desert finds			Daraj 014 rim	Weathered troilite, Acfer 019 (Fig. 6b)			Silica, Acfer 019
	Mean (n = 46)	Max.	Min.	Mean (n = 3)	Point 1	Point 2	Point 3	Mean (n = 4)
SiO_2	3.5	7.8	0.2	1.4	14.7	13.2	2.6	91.7
MgO	0.3	1.0	0.0	0.1	0.4	0.4	0.4	0.2
Al_2O_3	0.1	0.6	0.0	0.1	1.0	0.9	0.9	n.a.
CaO	0.4	1.9	0.0	n.a.	2.0	1.7	2.0	0.7
SO_2	1.0	3.5	0.4	1.0	0.2	0.3	0.2	n.a.
Cl	1.0	3.0	0.1	15.9	0.5	0.4	0.3	n.a.
Fe_2O_3	75.9	84.1	58.4	75.2	69.7	70.9	79.3	0.5
NiO	4.6	15.3	0.6	4.3	0.6	0.8	0.8	n.a.
Total	86.8	—	—	98.0	89.1	88.6	86.5	93.1

Max. and min. denote the maximum and minimum values respectively for each oxide or element. n.a. denotes not analysed.

4.3. Antarctic Finds

4.3.1. Petrography of Weathered Meteorites

Most of the Antarctic finds have much greater terrestrial ages than 'hot' desert meteorites, although their degrees of weathering as measured by Mössbauer spectroscopy are comparable (Table 2). Petrographic characteristics of the Antarctic finds are summarised in Table 2. In common with the 'hot' desert meteorites, they show a progressive thickening of Fe-oxide/oxyhydroxide rims around Fe,Ni metal grains and occlusion of intragranular pores as weathering proceeds (Table 2, Fig. 8). From petrographic data, occlusion of intragranular pores is essentially complete by the time that ~13 to 23% of the initial Fe^0 and Fe^{2+} has been oxidised (Table 2). In contrast to the 'hot' desert finds, Antarctic meteorites have no evidence for dissolution at the scale of the BSE images and very little

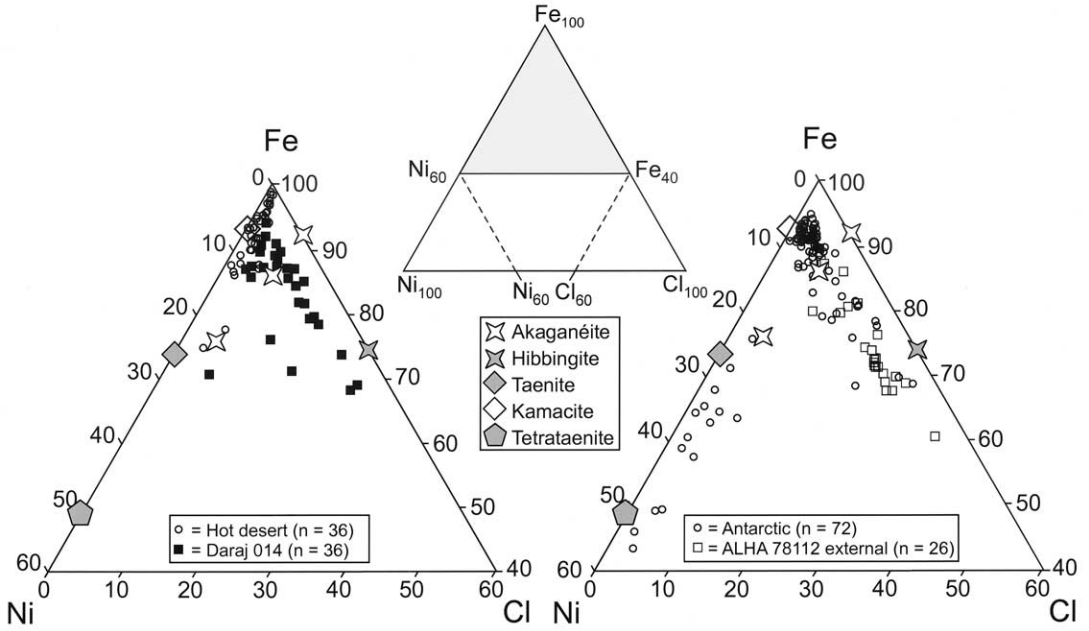

Fig. 4. Ternary diagrams illustrating the chemical composition of weathering products from 'hot' desert and Antarctic finds plotted as ratios of Fe, Ni and Cl (wt.% element). The 36 analyses of undifferentiated 'hot' desert meteorites include Acfer 263 (7 points), Billygoat Donga (16 points), Acfer 019 (3 points) and Acfer 298 (10 points). The Daraj 014 data, which are plotted separately, were taken from the traverse across the heavily weathered kamacite grain in Figure 2. The 72 analyses of undifferentiated Antarctic meteorites include ALH 77001 internal and external (10 points from each), ALH 77180 (14 points), ALH 78104 internal (12 points), ALH 78104 external (15 points) and ALH 77002 (11 points). Also plotted in the ternary diagrams are the ideal compositions of hibbingite and tetrataenite and the compositions of kamacite and taenite in L6 finds (from EPMA acquired during this study). The three compositions of akaganéite plotted represent an ideal Ni-free composition, the typical composition of akaganéite found by Buchwald and Clarke (1989) (86.7 wt.% Fe, 7.3 wt.% Cl, 6.0 wt.% Ni, ignoring O_2 and H_2O) and the most Ni-rich akaganéite found by Buchwald and Clarke (1989) (76 wt.% Fe, 4 wt.% Cl, 19 wt.% Ni, ignoring O_2 and H_2O).

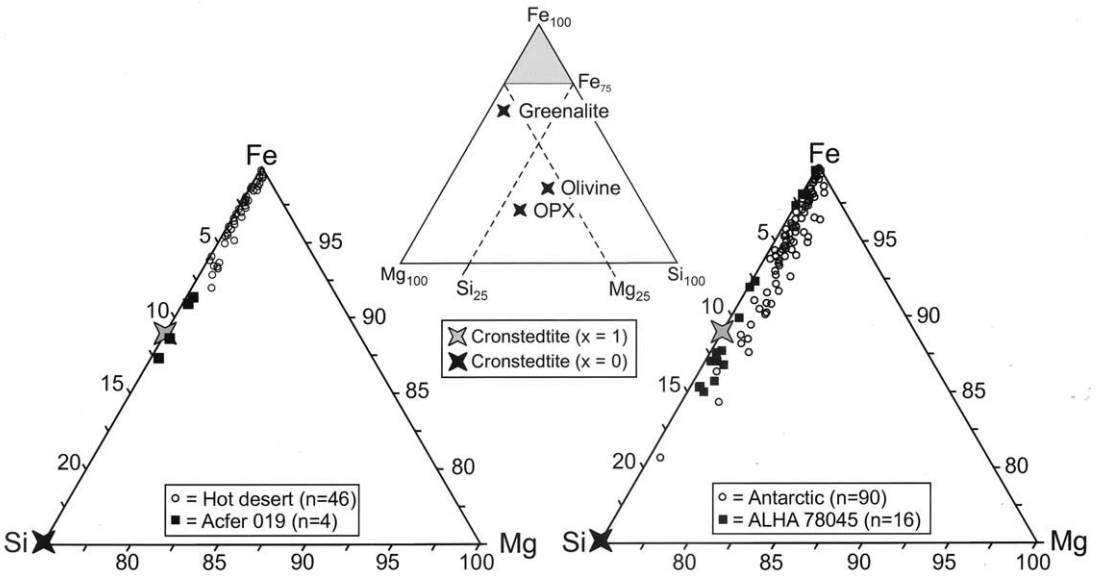

Fig. 5. Ternary diagrams illustrating the chemical composition of weathering products from 'hot' desert and Antarctic finds plotted as ratios of Si, Mg and Fe (wt.% element). The 46 analyses of undifferentiated 'hot' desert meteorites include Acfer 263 (7 points), Daraj 014 (10 points, none taken from the traverse in Fig. 2, Billygoat Donga (16 points), Acfer 019 (3 points) and Acfer 298 (10 points). The four separate Acfer 019 data points are from discrete silicate weathering products. The 90 analyses of undifferentiated Antarctic meteorites include ALH 77001 internal and external (10 points from each), ALH 77180 (14 points), ALH 78104 internal (12 points), ALH 78104 external (15 points), 78112 external (3 points), 78112 internal (15 points) and ALH 77002 (11 points). Included on the two ternary diagrams are the two points where cronstedtite of end-member compositions should plot (i.e., if $x = 1$and $x = 0$ in the cronstedtite formula). The three points in the central ternary diagram are compositions of greenalite (data from Newman and Brown, 1987) and olivine and orthopyroxene (OPX) found in L6 ordinary chondrites (data from this study).

evidence for brecciation accompanying weathering, although it is possible that brecciated outer parts of the finds may have been removed by katabatic winds. Additionally, very little weathered troilite was found and overall the Antarctic meteorites have a smaller mineralogical range of weathering products (Table 2). The six Antarctic finds studied here can be divided into two groups on the basis of the chemistry and mineralogy of their weathering products. The four least-weathered meteorites are dominated by Fe-oxide/oxyhydroxides which form rims to Fe,Ni metal grains and occlude intergranular pores. By contrast Fe,Ni metal rims and intergranular vein fills in the two most heavily weathered meteorites, ALHA 78045 and ALHA 77002, are predominantly composed of hydrous Fe-silicates.

4.3.2. Chemical Composition of Fe-Rich Weathering Products

Fe-rich weathering products in the four least-weathered meteorites are predominantly composed of Fe_2O_3, NiO, SiO_2 and Cl, with $< \sim 2$ wt.% of MgO, CaO and SO_2 (Table 4). Note the differences in mean chemical compositions of weathering products between internal and external samples of ALHA 77001 and 78104 (Table 4). Insufficient data were available to make meaningful comparisons between internal and external samples of the two other meteorites. Fe/Ni ratios of the weathering products vary over a wide range (Fig. 4). The Fe/Ni ratio of taenite grains ($\sim$2.1) is much lower that of their weathering products (Fe/Ni = $\sim$20–25, $\sim$2–3 wt.% NiO) whereas the Fe/Ni ratio of kamacite grains ($\sim$14) is in general comparable to that of their alteration products (Fe/Ni = $\sim$9–18, $\sim$3–9 wt.% NiO). A notable exception to this is the group of analyses with very low Fe/Ni ratios, the lowest of which are comparable to that of tetrataenite, Fe_1Ni_1 (Fig. 4). These high-Ni analyses are from four finds, ALH 77001 internal (1 data point), ALH 78104 external (3 data points, Table 4), ALH 78112 internal (1 data point) and ALH 77002 (10 data points). The analyses of Ni-rich weathering products from ALH 78104 (Table 4) are notable in having low analytical totals, indicating that the weathering products are hydrous, and probably porous, and also that the nickel does not come from very fine inclusions of a Ni-rich metal. In ALH 78112 the Fe,Ni metal grains that are surrounded by these Ni-rich weathering products are composed of a fine-scale intergrowth of Ni-rich and Ni-poor Fe,Ni metal (Figs. 8c and 8d). Semiquantitative X-ray microanalysis shows that the Ni-rich metal has near-equal proportions of Fe and Ni, consistent with tetrataenite (Fig. 8e), whereas the Ni-poor metal with which it is intergrown has very low Ni concentrations, and is probably kamacite. The interface between the outer surfaces of these Fe,Ni metal grains and the weathering products is irregular with the micrometre-sized tetrataenite lamellae standing proud of the more rapidly weathering low-Ni (?kamacite) lamellae (Fig. 8d). The alteration products have a similar Fe/Ni ratio to tetrataenite (Fig. 8e).

Despite the lack of petrographic evidence for weathering of troilite, Antarctic weathering products do contain measurable concentrations of sulphur ($\sim$0.6–2.1 wt.% SO_2, Table 4). Average concentrations of Cl are significantly greater in the Ant-

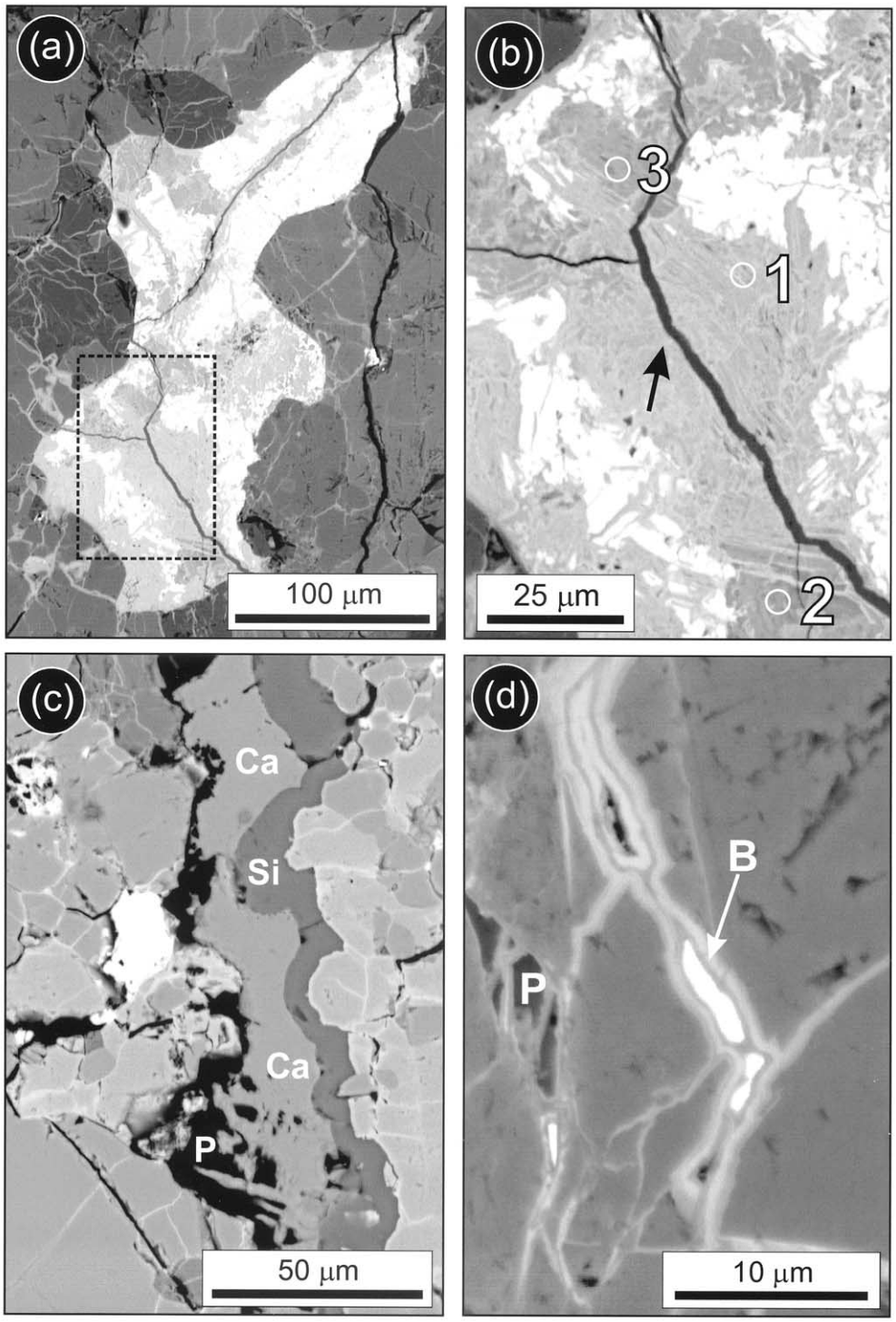

Fig. 6. BSE images of the weathered interiors of 'hot' desert meteorites. (a) A partially weathered troilite grain surrounded by olivine and orthopyroxene from Acfer 019. Remaining troilite is white whereas weathering products are light grey. (b) Image of the boxed area in (a). This image shows that volumes of a material with a relatively low mean atomic number (dark grey) are intergrown with the Fe-rich weathering products (light grey) and remaining troilite (white). The locations of three EPMA analyses are indicated. Data from them are listed in Table 3 and show that weathering products analysed at points 2 and 3 are Si-rich. The altered grain is cross-cut by a narrow vein of Ca-carbonate (arrowed). (c) BSE image of Acfer 019 showing a fracture (oriented north-south in the image) that contains a silica-rich compound (Si) and Ca-carbonate (Ca). Some porosity (P) also remains. Data from an EPMA analysis of the silica-rich compound are listed in Table 3. (d) A partially barite-filled vein in Acfer 298. Barite (B, arrowed) occurs in the centre of the vein, which is also lined by Fe-oxide/oxyhydroxides. Note that some porosity remains in the center of other parts of the vein and that a pore (P) has also been produced by dissolution of surrounding silicates.

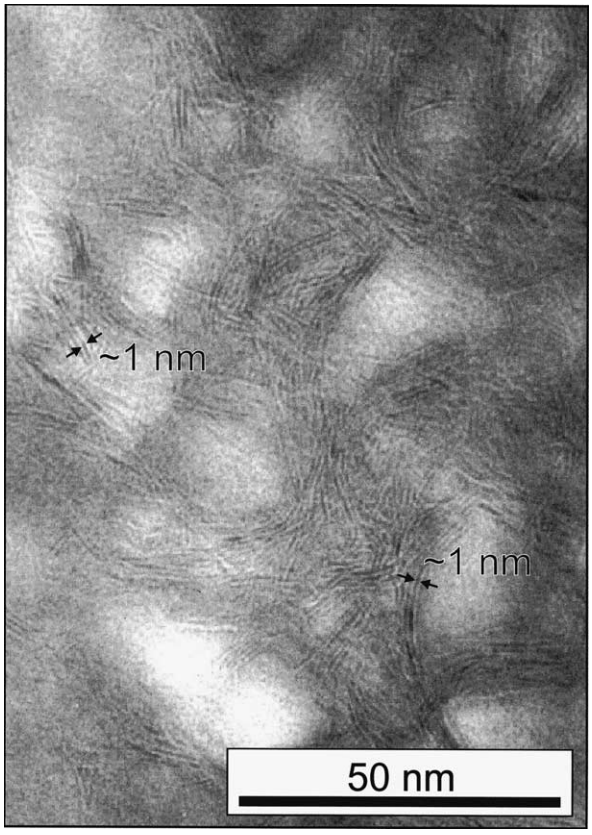

Fig. 7. High-resolution TEM image of weathering products within Billygoat Donga showing a pore between orthopyroxene grains that is occluded by subcircular aggregates of a mineral with a ~1 nm lattice fringe spacing.

arctic weathering products than in those from 'hot' deserts excluding Daraj 014 (Fig. 4) and importantly, weathering products in the external samples of ALHA 77001 and 78104 both have greater mean concentrations of Cl than corresponding internal samples (Table 4). EPMA analysis of a group of three pseudomorphs of Fe,Ni metal grains from the external sample of ALHA 78112 (mean composition listed in a separate column of Table 4) show that these weathering products have very high Cl concentrations. These data are also plotted separately in Figure 4. Note from Figure 4 that the most Ni-rich weathering products all have low Cl concentrations.

Si and Mg concentrations in Fe-rich Antarctic weathering products are on average greater than those from 'hot' deserts (Fig. 5, Table 4). In common with the 'hot' desert finds there is a positive correlation between SiO_2, MgO and CaO (Fig. 9), but a weaker negative correlation between SiO_2 and Fe_2O_3. Importantly, the mean SiO_2 concentration of Fe-rich weathering products in the four least-weathered Antarctic meteorites decreases with increasing terrestrial weathering and CaO, MgO show similar trends (Table 4). The sample containing weathering products with the greatest average SiO_2 concentrations (ALHA 77001 internal) has experienced the least amount of terrestrial weathering. Note the very significant difference between the internal and external samples of ALHA 77001 with regard to SiO_2 (Table 4).

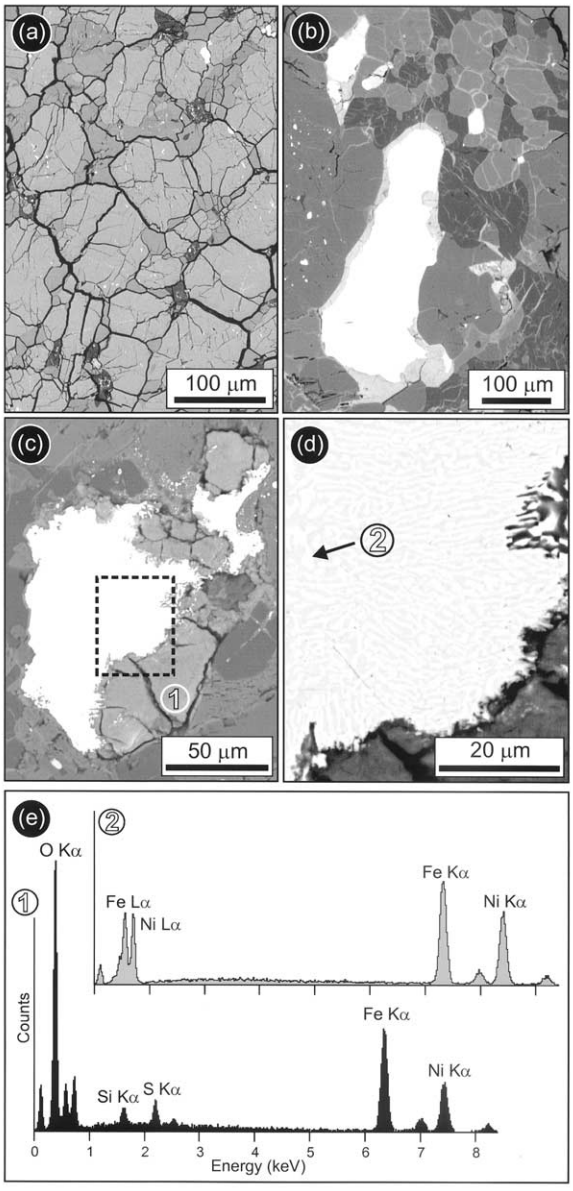

Fig. 8. BSE images and analytical data from ALHA 78104 external (a and b) and ALH 78112 internal (c–e). (a) An area of ALHA 78104 completely free of weathering products, demonstrating the abundance of primary intra and intergranular pores (black). Digital image analysis of this field of view shows that it has 18% porosity. (b) Part of the same thin section of ALHA 78104 showing Fe, Ni metal grains (white) that have been partially weathered, producing Fe-oxide/oxyhydroxide rims (light grey). These weathering products have also occluded those primary pores within a few hundred micrometres of the Fe,Ni metal grains to produce veins (lower right hand side of the image). (c) BSE image of a partially weathered Fe,Ni metal grain from ALH 78112. Most weathering products have formed in the lower and upper right hand sides of the grain. 1 denotes the location of an X-ray analysis in (e). (d) Higher magnification image of the boxed area in (c) illustrating the exsolution textures of the Fe,Ni metal. The partially weathered edge of the metal grain (upper right hand side) shows that lamellae of the low-Ni metal have weathered faster than the high-Ni metal. 2 denotes the location of an X-ray analysis in (e). (e) Two X-ray spectra of the partially weathered Fe,Ni metal grain from ALH 78112 in (c) and (d). Analysis 1 is of the weathering products and 2 is from a Ni-rich part of the exsolution microtexture. Note that the Ni-rich exsolved area and weathering products have similar Fe/Ni ratios.

Table 4. Average chemical compositions of Fe-rich weathering products in the four least-weathered Antarctic finds determined by EPMA.

	ALH 77001			ALH 78104				
	Internal	External	ALH 77180	Internal	External	ALH 78112	ALH 78104 Ni-rich[a]	ALH 78112 PM[b]
SiO_2	10.9	4.0	5.7	2.2	3.5	2.6	3.1	1.1
MgO	1.5	1.0	0.7	0.5	0.7	0.7	1.2	0.9
CaO	0.5	0.1	0.2	n.da	0.2	0.1	0.1	0.2
SO_2	0.6	2.1	0.6	2.1	0.9	0.8	1.2	0.9
Cl	1.2	8.7	3.4	2.3	3.0	3.0	2.3	12.8
Fe_2O_3	64.1	68.9	77.8	74.1	71.7	73.7	48.0	72.1
NiO	5.7	5.7	4.5	4.2	8.1	5.2	23.6	5.2
Total	85.4	90.5	92.9	85.4	88.1	86.1	79.5	93.2
n	10	10	14	12	15	18	3	26

Internal and external denote the part of the meteorite from where the sample studied was taken.
[a] An average of three analyses of Ni-rich weathering products from the external sample.
[b] Pseudomorphs of Fe,Ni metal grains. Al_2O_3 is not quoted as concentrations in all cases were below detection limits. n.a. denotes not analysed. n denotes number of analyses.

4.3.3. Weathering Products in ALHA 78045 and 77002

These meteorites differ from the other four Antarctic finds in the mineralogy and chemical composition of their weathering products; they also have the greatest terrestrial ages of the six Antarctic finds analysed. The intra and intergranular veins in ALHA 78045 (Fig. 10a) are largely filled with weathering products comprising micrometre-scale intergrowths of Fe-oxide/oxyhydroxides with Fe-silicates (Figs. 10b and 10c). Some of the veins are filled by Fe-silicate fibres $\leq \sim 1$ μm in width by ~ 10 μm in length (Figs. 10c and 10d). The veins also have evidence for localised brecciation (Fig. 10c). Veins in ALHA 77002 are similar in appearance but the volumes Fe-oxide/oxyhydroxide and Fe-silicate are intergrown on a finer scale (Figs. 10e and 10f). In addition, the majority of the most Ni-rich weathering products analysed by EPMA (Fig. 4) are from ALH 77002. This meteorite is more brecciated than ALHA 78045 (Fig. 10e), but the effects are again localised. EPMA work concentrated on the Fe-silicate veins in ALHA 78045 because these veins are wider than in ALHA 77002 and the intergrowths are sufficiently coarse so that the Fe-silicate can be readily distinguished from Fe-oxide/oxyhydroxide (e.g., Fig. 10c). These data show that the Fe-silicate weathering products have mean and maximum SiO_2 concentrations of 14.7 and 17.3 wt.% respectively (Table 5) and Fe/Si/Mg ratios are comparable to those of the most Si-rich weathering products from the four less-weathered Antarctic finds (Fig. 5).

Many of the Fe,Ni metal (taenite) grains in ALHA 78045 display a different style of weathering to metal grains in most

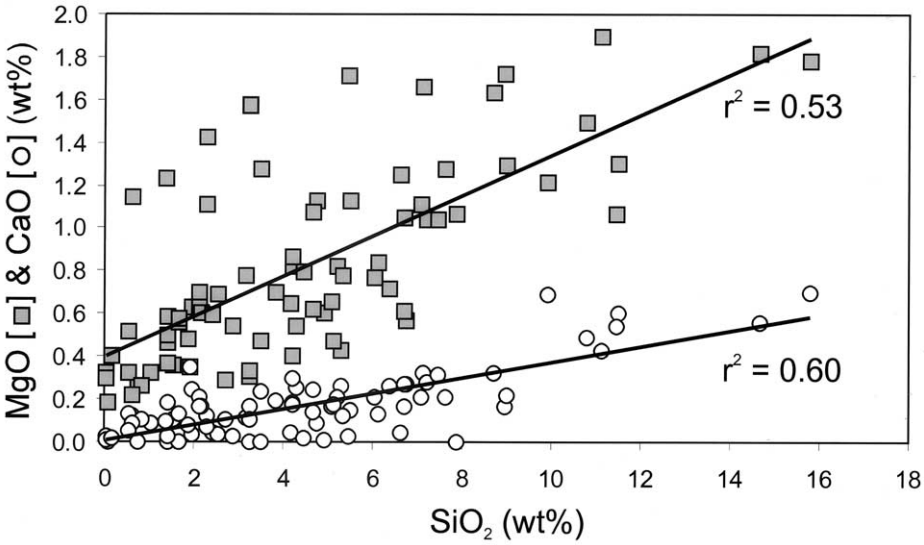

Fig. 9. Plot of SiO_2 against MgO and CaO from EPMA analyses of Fe-oxide/oxyhydroxide dominated weathering products within Antarctic finds. Regression lines for the two datasets are shown, together with correlation coefficients. Both datasets have 79 points that are from ALH 77001 internal and external (10 points from each), ALH 77180 (14 points), ALH 78104 internal (12 points), ALH 78104 external (15 points), 78112 external (3 points) and 78112 internal (15 points). These data exclude analyses from ALHA 78045 and ALHA 77002 owing to the common intergrowth of the Fe-oxide/oxyhydroxides with coarsely crystalline Fe-silicates.

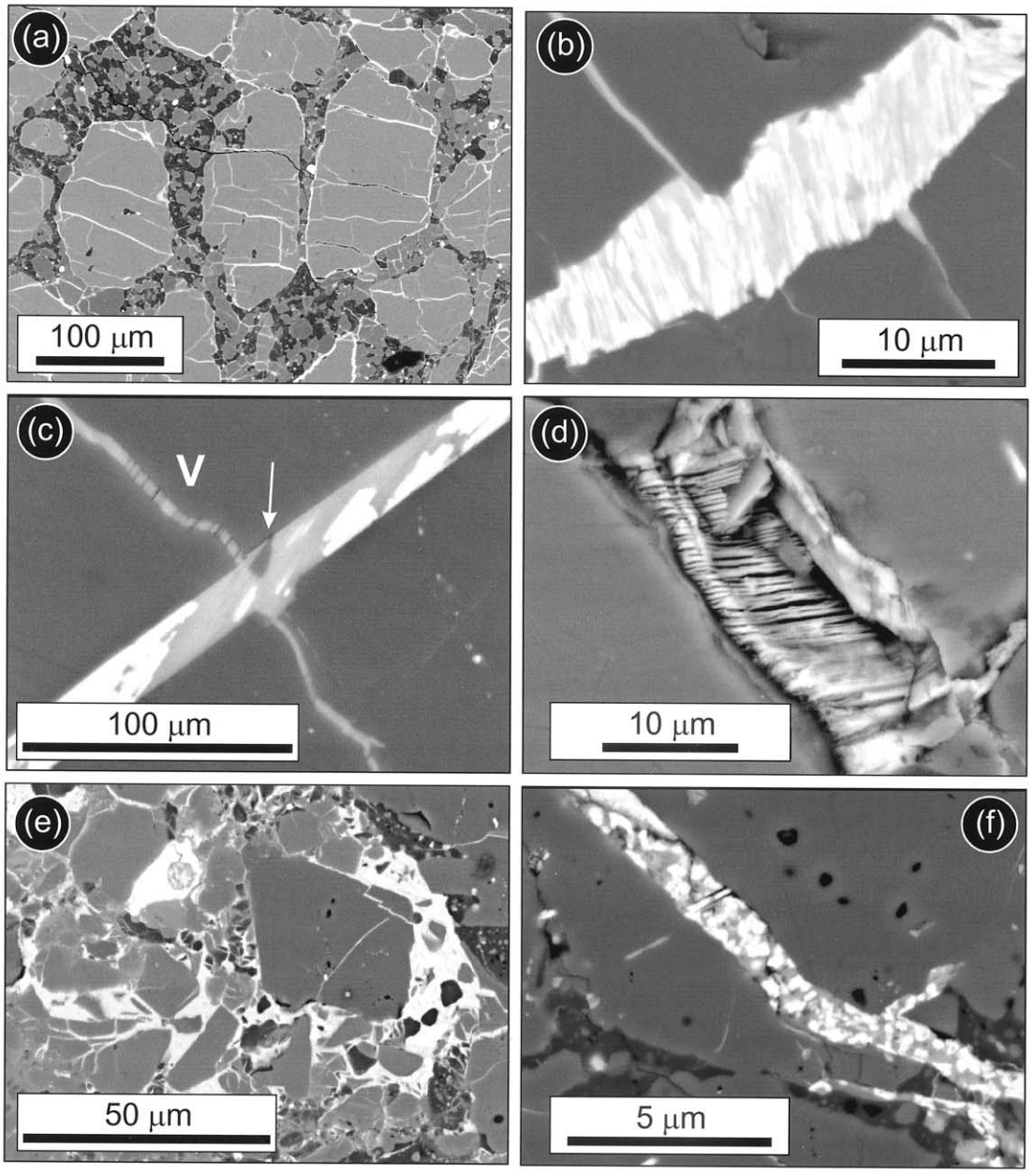

Fig. 10. BSE images of ALHA 78045, (a) to (d) inclusive, and ALHA 77002, (e) and (f). (a) In this field of view veins occluded by weathering products predominantly occur within the coarse euhedral olivine grains rather in the more finely crystalline feldspathic groundmass. (b) An intragranular fracture that is occluded by a sub-μm scale lamellar intergrowth of Fe-oxide/oxyhydroxide (white) and Fe-silicate (light grey). (c) An intragranular vein occluded by a coarser scale intergrowth of Fe-oxide/oxyhydroxide (white) and Fe-silicate (grey). Note the fibrous habit of Fe-silicate that occludes the narrower vein (V) that is oriented perpendicular to the main one. In addition a small fragment of olivine (arrowed) has been displaced during dilation of the fracture, possibly accompanying the precipitation of weathering products. (d) A broken surface of a vein revealing the fibrous habit of the Fe-silicate fill. (e) Breccia of olivine, orthopyroxene and feldspar that is cemented by Fe-silicate (lower left hand side) and a very fine-scale intergrowth of Fe-silicate with Fe-oxide/oxyhydroxide (middle right hand side). (f) Intragranular vein (oriented NW-SE) containing a patchy intergrowth of Fe-silicate (grey) with Fe-oxide/oxyhydroxide (white).

of the other meteorites studied. Instead of forming a concentric rim, the weathering products have replaced patches of grain interiors (Fig. 11). Most of the taenite altered in this way displays an inner zone of partial alteration and outer zone of more intense alteration. The inner zone is typically enriched in O, Si and Ni and depleted in Fe relative to taenite (Fig. 11b). Fe,Ni metal that remains within this zone display a complex microtexture (Figs. 11a and 11b) which comprises narrow rods

Table 5. Chemical composition of hydrous Fe-silicate weathering products in ALHA 78045, determined by EPMA, and comparison with previously described meteorite weathering products.

	Fe-silicate vein fills		EETA 79005	Alteration products of Fe,Ni metal (taenite)			Pecoraite
				Figure 11b		Figure 11a outer zone (mean, $n = 3$)	
	Mean[a]	Maximum Si[b]	Gooding (1986)[c]	Inner zone, greatest Si[b]	Outer zone, greatest Si[b]		Faust et al. (1969)
SiO_2	14.7	17.3	19.2	3.5	11.4	28.5	31.0
MgO	0.6	0.5	5.6	n.d.	0.9	3.4	0.5
Al_2O_3	0.4	0.5	7.7	n.d.	1.2	n.d.	1.4
CaO	0.5	0.2	0.1	n.d.	0.3	0.7	0.4
SO_2	0.1	0.1	2.2	0.7	2.0	0.2	n.s.
Cl	0.6	n.a.	0.8	n.a.	n.a.	n.a.	n.s.
Fe_2O_3	70.7	69.6	61.6	—	—	—	—
FeO	—	—	—	55.2	23.1	34.2	0.7
NiO	1.9	1.1	<0.1	51.8	34.4	15.9	51.5
Fe/Ni[d]	33.2	56.6	>539	1.1	0.9	2.1	0.0
Total	89.5	89.3	97.3	112.3[e]	74.2	85.0	85.5

[a] Mean of 11 analyses with > 10 wt.% SiO_2. [b] Analysis with the greatest Si concentration. [c] Includes 2.2 wt.% K_2O and 0.46 wt.% P_2O_5 and sulphur was expressed as SO_3. [d] Fe/Ni of taenite = ~2.3. [e] High total indicates that a proportion of the iron and nickel is present as metal. n.a. denotes not analysed. n.d. denotes not detected. n.s. denotes not stated by the authors.

of taenite in a kamacite matrix. The outer zone of alteration in ALH 78045 taenite has no surviving Fe,Ni metal and has a characteristically 'cracked' appearance in BSE images (Figs. 11a and 11b). This material is enriched in O and Si and depleted in Fe and Ni relative to both the inner zone alteration products and surviving taenite. Data from EPMA analyses of the inner and outer zone alteration products are listed in Table 5. These data confirm that the weathering products are very different in bulk chemical composition to the other Fe-silicates from ALHA 78045.

High-resolution TEM images of ALHA 78045 and ALHA 77002 show that nanometre-sized crystallites of a mineral with a ~1.0 nm lattice fringe spacing occlude fractures within olivine and orthopyroxene grains (Fig. 12a). These crystallites are described and illustrated in more detail by Bland et al. (2000b). Wider fractures in ALHA 77002 are partially occluded by columnar aggregates of relatively coarse (~30 × 100 nm) lath-shaped crystals that are oriented with their long axes perpendicular to fracture walls (Fig. 12b). High-resolution images and SAED patterns show that these crystals predominantly have a ~0.7-nm basal layer spacing, but narrow interstratifications of a mineral with a ~1.0 basal layer spacing also occur (Figs. 12b and 12c).

5. DISCUSSION

5.1. Weathering of Ordinary Chondrite Falls

The significant volumes of alteration products of Fe,Ni metal and troilite in New Concord illustrate how rapidly equilibrated ordinary chondrites can react with the terrestrial environment, even when stored under museum conditions. These observations are in agreement with Consolmagno et al. (1999), who suggested that most 19th century falls will show some effects of terrestrial weathering. The presence of two generations of alteration products in New Concord, distinguished by Fe/O ratios, suggests that the alteration is multiphase. Alteration products in the inner discontinuous layer, which have relatively low Fe/O ratios, may themselves recrystallize to the more abundant alteration products in the outer layer, which have a greater Fe/O ratio. The presence of rimmed Fe,Ni metal grains and partially occluded veins in New Concord demonstrates that intergranular pores do not have to be completely filled with liquid water in order for extensive alteration to take place. As discussed in later sections the host of Si within these weathering products is difficult to determine but could be clays or phyllosilicates.

5.2. Contrasts Between Hot Desert and Antarctic Weathering

This work has demonstrated that there are a number of similarities but also important differences between processes and products of terrestrial weathering of ordinary chondrites in 'hot' deserts and Antarctica. Weathering in both environments is dominated by the alteration of Fe,Ni metal to a range of Fe-oxides and oxyhydroxides. In addition to replacing the Fe,Ni metal, these minerals occlude primary intergranular pores, producing a network of veins. In 'hot' deserts, troilite weathers at a comparable or slightly slower rate than Fe,Ni metal, but there is a very little evidence for weathering of troilite in the Antarctic meteorites. These differences in the susceptibility of troilite to weathering, which were also noted by Ruzicka (1995), may simply be due to contrasts in average temperatures between the 'hot' and cold desert environments (A. Bevan, personal communication, 2002). Contrasts in the petrography of weathered meteorites between the two environments include abundant evidence for brecciation and dissolution in 'hot' desert meteorites but very little evidence for either process in Antarctic finds. The greater brecciation of 'hot' desert finds may be due to more rapid and destructive volume changes than experienced by Antarctic finds, especially for those meteorites that fell during relatively wet periods (A. Bevan, personal communication, 2002). Significant differences

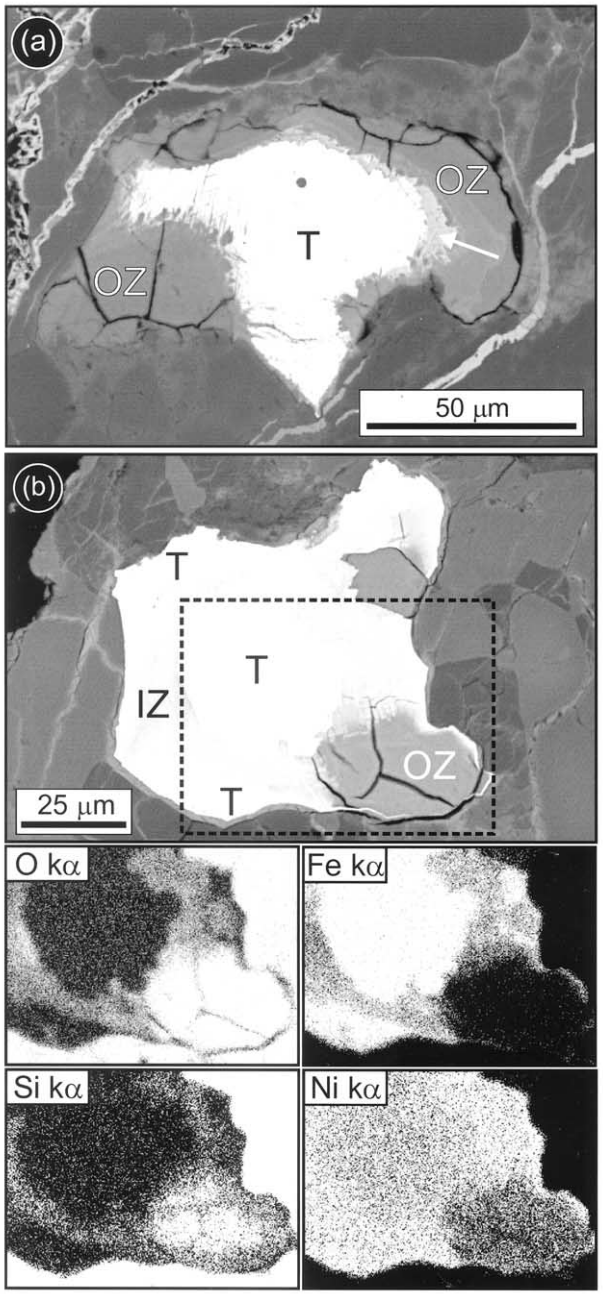

Fig. 11. Images of weathered Fe,Ni metal (taenite) grains from ALHA 78045. (a) BSE image of a taenite (T) grain that has a very narrow inner zone of alteration (arrowed) and a wider outer zone (OZ). Note the fractures within the outer zone weathering products and lamellar structures at the interface between weathering products and remaining metal. (b) BSE image of a partially weathered taenite grain and corresponding X-ray maps of four elements (below) taken from the boxed area of the image. The BSE image shows that taenite (T) remains in the center and around parts of the margins of the grain. Most of the taenite has been partially altered to form an inner zone (IZ) that the X-ray maps show is enriched in O, Si and Ni and depleted in Fe relative to the taenite. A small patch of characteristically fractured outer zone (OZ) alteration can be seen on the lower right hand edge of the grain in the BSE image. This zone is enriched in Si and O but depleted in both Fe and Ni relative to the inner zone and precursor taenite.

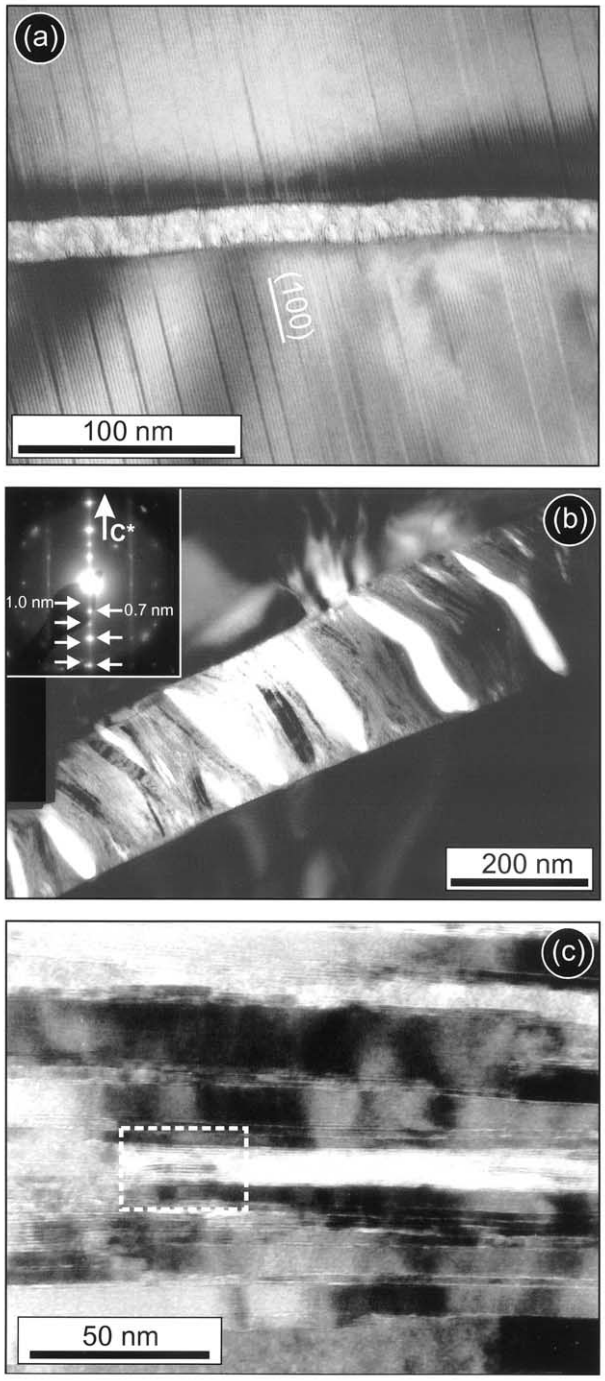

Fig. 12. TEM images of weathering products from ALHA78045 and 77002. (a) An orthopyroxene grain from ALH 78045 that is cross-cut by a fracture (oriented east-west in the image). The fracture is occluded by very small crystallites of a mineral with a ~1 nm basal spacing that have nucleated on terminations of the ~1.8 nm (100) lattice planes of orthopyroxene. (b) Pillar-shaped aggregates of ~100 nm-long phyllosilicate crystals bridging a ~200 nm-wide intragranular fracture in ALH 77002. A SAED pattern of one of the strongly-diffracting phyllosilicate crystals (inset) shows two sets of reflections, a major set with a ~0.7 nm spacing and a subsidiary set with a ~1.0 nm spacing. Note that the SAED pattern is not correctly oriented relative to the diffracting crystals. (c) High-resolution image of a phyllosilicate crystal from ALH 77002. The majority of lattice fringes have a ~0.7 nm spacing but interstratifications with a ~1.0 nm spacing (boxed area) also occur.

are also apparent between the two environments with regard to the chemical and mineralogical composition of weathering products. The mineralogical variety of 'hot' desert weathering products is considerable and in addition to Fe-oxide/oxyhydroxides includes Fe-poor sulphates, carbonates and silica whereas almost all weathering products of Antarctic meteorites are Fe-rich. The chemical compositions of Fe-oxide/oxyhydroxides also differ between 'hot' desert and Antarctic meteorites, especially with regard to Si and Cl concentrations. Potential reasons for differences in terrestrial weathering between the two environments are discussed below.

Climatic contrasts between 'hot' and cold deserts are obviously considerable, although there are some similarities. Both environments are typically arid, which accounts for their usefulness as meteorite collection areas. Air temperatures on the Antarctic plateau are permanently below freezing, but liquid water can exist under certain conditions. Cassidy et al. (1992) notes that some meteorites are recovered from pools of water and icicles on meteorite surfaces indicate that melting and refreezing of ice has taken place. Using temperature sensors within an unweathered meteorite fall (Allende) placed on Antarctic blue ice, Schultz (1986, 1990) found that over a 21-day period from December 1985 to January 1986 the temperature within the meteorite was consistently ~5°C greater than air temperature (~−10 and −15°C respectively). However, for only a couple of days during this time, when wind speeds were low, did the temperature within the meteorite rise above 0°C and up to +5°C. However, it is possible that the meteorite can still be weathered when internal temperatures are subzero, by the action of 'unfrozen water' (Gooding, 1986), and low-albedo meteorite may be warmed by solar radiation even when buried several metres beneath the ice (Harvey and Score, 1991). Climatic conditions in Saharan meteorite collection areas are summarised by Ash and Pillinger (1995). They show that mean annual air temperatures range from ~22 to 25°C and precipitation is 8 to 43 mm yr^{-1}. However as Ash and Pillinger (1995) emphasise, little of this moisture will be available for weathering owing to high rates of evaporation. They also note that the durinal temperature range in these environments can be > 35°C, falling to subzero at night and given the low albedo of the meteorites it is possible that their internal temperatures could approach the boiling point of water on the hottest days. It is important to note that climate in the Sahara and Nullarbor has changed during the terrestrial history of the meteorites (Bland et al., 1998b, 2000b; Lee and Bland, 2003). Thus, the present-day climate is not necessarily a good indication of the conditions under which the 'hot' desert meteorites have spent most of their terrestrial life. Bland et al. (1998b) have found good evidence that the Sahara and Nullarbor have both been more humid at times during the last ~30 ka and meteorites were more intensively weathered during those periods.

5.3. Mineralogy and Chemistry of Fe-Oxides and Oxyhydroxides

We did not undertake a comprehensive study of the mineralogy of Fe-oxide/oxyhydroxide weathering products. However, Buchwald and Clarke (1989) found that the principal weathering products of Fe,Ni metal (both kamacite and taenite) in Antarctic iron meteorites and ordinary chondrites were akaganéite and goethite with smaller volumes of lepidocrocite and maghemite. Zolensky and Gooding (1986) reported hydronium jarosite and geothite from ALHA77003, an Antarctic C3 find.

Fe-oxide/oxyhydroxides in 'hot' desert and Antarctic finds contain considerable concentrations of Ni. In both environments weathering products of kamacite have similar Fe/Ni ratios to the precursor grain, and a comparable relationship was found by Buchwald and Clarke (1989). However, weathering products of taenite tend to have greater Fe/Ni ratios than the metal grain, indicating that most Fe-oxide/oxyhydroxides can only accept a certain proportion of Ni within their crystal structures. This is in agreement with Buchwald and Clarke (1989) who found the following concentrations of Ni in weathering products: akaganéite 0.5 to 19 wt.%, goethite 1 to 8 wt.%, lepidocrocite 0.5 to 11 wt.% and maghemite 0.4 to 7 wt.%. Thus it is likely that nickel is removed in solution from sites of active weathering and a similar process was described by White et al. (1967), who noted that terrestrial weathering products in the 'hot' desert Wolf Creek iron meteorite had lower concentrations of nickel than the precursor minerals. They suggested that the nickel had remained in its divalent state to be removed in solution whereas the iron was oxidised to its ferric state and precipitated, predominantly as goethite and Ni-maghemite.

The Fe-oxide/oxyhydroxide weathering product with greatest concentrations of Ni found by Buchwald and Clarke (1989) was akaganéite (0.5–19 wt.% Ni). The analysis with 19 wt.% Ni (expressed on a O_2- and H_2O-free basis) was from adjacent to a grain of troilite with a Fe/Ni ratio of ~4. However, this analysis has considerably lower Ni concentrations than the most Ni-rich weathering products found in this study, which had formed on grains composed of an intergrowth of tetrataenite with ?kamacite (Figs. 4 and 8, Table 4). The mineralogy of these Ni-rich Fe-oxide/oxyhydroxides is not known, but it may be significant that the three akaganéite analyses from Buchwald and Clarke (1989) that are plotted in Figure 4 define a line of decreasing Fe and Cl concentrations with increasing Ni. The most Ni-rich analyses from Antarctic finds analysed for this study plot close to the akaganéite line if extended to greater Ni and lower Fe and Cl concentrations. Thus the Ni-rich minerals may be Ni analogs of akaganéite.

Sulphur must be very mobile during weathering in 'hot' deserts because weathering products within troilite pseudomorphs have very low sulphur concentrations. The average concentration of sulphur in weathering products of Fe,Ni metal (~1 wt.% SO_2) is probably insufficient to account for all of the sulphur liberated from troilite and so some sulphur must be lost from the meteorite. Ruzicka (1995) estimated that ~20% of the sulphur initially within Nullarbor 018 (L6) had been removed from the meteorite in solution during weathering. Importantly, weathering products in Antarctic meteorites contain ~1 to 2 wt.% SO_2, comparable to those in 'hot' desert meteorites, despite the lack of petrographic evidence for troilite weathering. It is possible that the sulphur, in common chlorine, is derived from outside the meteorite (see below).

The range of chlorine concentrations in Fe-oxide/oxyhydroxide weathering products is considerably greater in Antarctic than 'hot' desert finds, apart for Daraj 014, which has a comparable range of Cl concentrations and Fe/Cl ratios to the Antarctic meteorites within a single layered rim (Figs. 2 and 4). Previous work has shown that two Cl-bearing minerals may

form by weathering of meteorites. Akaganéite contains 0.3 to 5.4 wt.% Cl in Antarctic meteorites, although synthetic minerals may have up to 6.4 wt.% Cl (Buchwald and Clarke, 1989). Hibbingite (β-$Fe^{2+}{}_2[OH]_3Cl$) ideally has ~18 wt.% Cl (Saini-Eidukat et al., 1994) and has been reported from a number of weathered iron meteorites where it can occur in association with akaganéite (Buchwald and Koch, 1995). By contrast, goethite, lepidocrocite and maghemite in Antarctic meteorites contain < 0.2 wt.% Cl (Buchwald and Clarke, 1989). In addition, it is possible that antarcticite ($CaCl_2 \cdot 6H_2O$) forms as a temporary weathering product in Antarctic environments (M. Zolenky, personal communication, 2002).

Most 'hot' desert meteorite weathering products have high Fe/Cl ratios (Fig. 4), indicating that akaganéite is rare. However, Daraj 014 is notable in containing Cl-rich weathering products. The concentrations of Cl indicate that these weathering products are likely to be akaganéite, although some points have even greater Cl concentrations, indicating that hibbingite also occurs (Figs. 2 and 4). The maximum concentration of Cl found by EPMA in this meteorite (21.5 wt.%, Fig. 2) suggest that a Fe-rich mineral with an even greater concentration of Cl than hibbingite may be present. On average Antarctic weathering products have greater concentrations of Cl than those from 'hot' desert meteorites (excluding Daraj 014) (Fig. 4). The Cl concentrations of most analyses are consistent with akaganéite with or without intergrowths of Cl-poor Fe-oxide/oxyhydroxides (Fig. 4), whereas other analyses, especially from ALHA 78112 external (Fig. 4), again indicate that hibbingite is present. In common with Daraj 014 a few points analysed have very high Cl concentrations (maximum of 27 wt.% Cl), suggestive of a mineral with a greater Cl/Fe ratio than hibbingite (Fig. 4). The Cl-rich analyses from both 'hot' desert and Antarctic meteorites define a line of relatively invariant Ni concentrations but a reciprocal relationship between Fe and Cl (Fig. 4). This trend is interpreted to represent intergrowths between the various Ni- and Cl-bearing Fe-oxide/oxyhydroxides.

Importantly, where both the internal and external samples of the Antarctic meteorites were analysed, weathering products in the external samples consistently have a greater average Cl concentration (Table 4). These data support the suggestion by Buchwald and Clarke (1989) that most of the Cl was derived from outside of the meteorite (the Antarctic atmosphere, cryosphere or hydrosphere). Chemical analyses of H5/6 Antarctic meteorites by Langenauer and Krähenbühl (1993) demonstrated that the concentration of Cl (and other halogens) decreases with depth below the meteorite's surface and that meteorites recovered further from the sea had less halogen contamination that those closer to the sea. These data are consistent with derivation of the halogens from air-borne seaspray (Langenauer and Krähenbühl, 1993). Shinonaga et al. (1994) concluded that the sequestration of Cl by Antarctic meteorites was aided by active weathering reactions in the interior of the meteorite. We have been unable to find any equivalent studies of halogen contamination in Saharan or other 'hot' desert finds so the provenance of Cl within weathering products in Daraj 014 remains uncertain. We fully recognise that we have examined an insufficient number of 'hot' desert meteorites to draw any firm conclusions about halogen contamination. The growth of halite speleothems in Nullarbor caves over the last 30 ka shows that chlorine is available in that environment (Goede et al., 1992), so more Nullarbor meteorites need to be examined to determine whether this chlorine has also been sequestered by meteorite weathering products.

Buchwald and Clarke (1989) demonstrated that Cl is very important in meteorite weathering because it plays a catalytic role in the alteration of Fe,Ni metal. An expression of this reaction, using a composition of akaganéite common in Antarctic meteorites, is as follows (from Buchwald and Clarke, 1989):

$$30Fe^0 + 2Ni^0 + 47O + 19H_2O + 4H^+ + 4Cl^- \quad \text{(kamacite)} \rightarrow 2[Fe_{15}Ni][O_{12}(OH)_{20}]Cl_2(OH) \quad \text{(akaganéite)} \qquad (1)$$

In this model the akaganéite subsequently transforms (or 'ages') to goethite and maghemite with loss of Cl. A prediction of this model would be that where thick weathering rims are present on Fe,Ni grains the Cl should be concentrated in those weathering products adjacent to remaining Fe,Ni metal. Results from the EPMA traverse of Daraj 014 in Figure 2 shows that Cl is indeed most abundant in the vicinity of the surviving Fe,Ni metal grain, although it is also concentrated in discrete layers away from the interface that represent the former edge of the Fe,Ni grain. Note that results from weathering experiments undertaken by Bland et al. (1997) suggested that Cl is not necessary for the stability of akaganéite. Thus, loss of Cl may not cause it to break down, or 'age' as Buchwald and Clarke (1989) have suggested.

5.4. Si-rich Weathering Products

5.4.1. Previous Descriptions of Si-rich Weathering Products in Meteorite Finds

Nearly all EPMA analyses of 'hot' desert and Antarctic weathering products have measurable concentrations of SiO_2, MgO and CaO, indicating that one or more silicate minerals may form during weathering. Note that the outer layer of weathering products of New Concord also contains Si (Fig. 1c). In a comprehensive review of the mineralogy of meteorite weathering products, Rubin (1997) lists four Si-bearing materials: illite, pecoraite, quartz and opal. The source of the description of illite and quartz is not stated, but the descriptions of pecoraite and opal are reviewed in later parts of this discussion. In addition, Si-rich weathering products have been described, although not unambiguously identified, by Gooding (1986) from a number of meteorites from the Alan Hills and Victoria Land areas of Antarctica. The chemical composition of weathering products from EETA 79005, termed ′sialic rust', is listed in Table 5. Gooding (1986) also identified volumes of smectite (or a mica-like phase) from a number of Antarctic meteorites. Most of this material was found within the fusion crusts but it also occurred within glass, maskelynite and plagiolcase in interiors of two stones. The general composition of this mineral is: $(K_{0.26},Ca_{0.04})(Al_{0.97},Ti_{0.02},Fe^{3+}{}_{0.77},Mg_{0.03})Si_{4.00}O_{10}(OH)_2 \cdot nH_2O$ (Gooding, 1986).

5.4.2. Mineral Host of Si, Mg and Ca Ions

Discrete silicate minerals were found intergrown with the Fe-oxide/oxyhydroxides in only three of the meteorites studied,

Acfer 019 (Table 3, Fig. 6) and ALHA 78045 and 77002. The mineralogy of these weathering products is discussed below. There are two possible hosts for the Si, Mg and Ca ions in Fe-rich weathering products from those 'hot' desert and Antarctic meteorites that lack discrete silicate minerals in BSE images. These ions could occur in direct association with the Fe-oxide/oxyhydroxide crystallites (i.e., adsorbed or substituted) or the Si, Mg and Ca could be present within one or more very finely crystalline silicate minerals intergrown with the Fe-oxide/oxyhydroxides. Reported concentrations of Si in association with Fe-oxyhydroxides vary over a wide range. For example, Herbert (1999) reported a mean concentration of 2 wt.% Si in Fe-oxyhydroxides from mine drainage-contaminated groundwater and Hochella et al. (1999) found Fe/Si ratios of ~6:1 in ferrihydrite, also from acid mine drainage. Boyd and Scott (1999) reported mean concentrations of 7.5 wt.% Si in 'two-line' ferrihydrite from the Franklin seamount, Papua New Guinea. They suggested that a shift in peaks from X-ray diffraction patterns indicated that the Si was substituted within the structure of the ferrihydrite. Thus it is possible that most or even all of the SiO_2 in Fe-rich meteorite weathering products occurs on, or within Fe-oxide/oxyhydroxide crystals. This possibility can only be adequately addressed by undertaking high-resolution chemical analyses by TEM, which are beyond the scope of the current study. The good correlation between SiO_2, MgO and CaO in Antarctic weathering products (Fig. 9) does however suggest that these ions may be present within a silicate mineral that has a Si/Mg/Ca ratio of ~1:0.2:0.1. High-resolution TEM images of Billygoat Donga, ALHA 78045 and 77002 showed that a very finely crystalline mineral with a ~1-nm lattice fringe spacing is commonplace within intragranular pores. A lattice fringe spacing of ~1 nm is consistent with collapsed smectite, or possibly a mica, although the absence of significant concentrations of Al or K in the EPMA analyses is inconsistent with either mineral as a host of the Si. In addition, the occurrence of the ~1.0-nm mineral within highly restricted intragranular pores in orthopyroxene, where it has a topotactic relationship to that mineral (Fig. 12a), indicates that significant element exchange has not taken place (Bland et al., 2000b). Thus, although the mineral with a ~1.0-nm lattice fringe spacing cannot be unambiguously identified, we suggest that it is the host to a proportion of the SiO_2, MgO and CaO in Fe-rich weathering products from 'hot' desert and Antarctic meteorites.

5.4.3. *Silicate Weathering Products in Acfer 019, ALHA 78045 and 77002*

Discrete grains of silicate mineral weathering products were identified in BSE images of only three meteorites, Acfer 019, ALHA 78045 and ALHA 77002. The more Si-rich analyses of these weathering products from Acfer 019 and ALHA 78045 are consistent with cronstedtite, a trioctahedral 1:1 layer silicate (Lee et al., 2003) (Fig. 5). This mineral belongs to the serpentine-kaolinite group (Hybler et al., 2000) and its formula is often expressed as $(Fe^{2+}_{3-x}Fe^{3+}_{x})(Si_{2-x}Fe^{3+}_{x}O_5)(OH)_4$ where $0 < x < 1$. The two ideal end-member compositions cronstedtite are also plotted in Figure 5. Studies of terrestrial cronstedtite show that $x = \sim 0.7$ to 0.8 (Hybler et al., 2000). TEM data from ALHA 77002 are also consistent with cronstedtite, both the lath-shape of the individual crystals (Fig. 12b) and the ~0.71-nm basal layer spacing in SAED patterns and high-resolution TEM images (Figs. 12b and 12c) ($d_{[001]}$ cronstedtite = 7.09 nm). It is possible that very fine-scale intergrowths of cronstedtite with Fe-oxide/oxyhydroxide are the host of Si and Mg in weathering products from the other 'hot' desert and Antarctic meteorites studied. It is interesting to note that cronstedtite from ALHA 77002 contains interstratifications of a mineral with a ~1.0-nm lattice fringe spacing (Figs. 12b and 12c). This could be the same mineral that occludes intra and intergranular pores in Billygoat Donga (Fig. 7) and ALH 78045 (Fig. 12a).

In addition to cronstedtite, ALHA 78045 contains Si-rich weathering products that have replaced Fe,Ni metal (taenite) grains. Partial alteration of the taenite has produced an inner zone of weathering products that contain relatively low concentrations of Si and O. Their high analytical totals (Table 5) indicate that much of the Fe and Ni within this zone is present as inclusions of Fe,Ni metal (taenite has an analytical total of ~130 wt.% if Fe and Ni are expressed as oxides). Thus, the inner zone is inferred to be an intergrowth of taenite with a Si- and O-bearing weathering product. The outer zone alteration products are even more enriched in Si, together with Mg and Ca and, from analytical totals, H_2O and depleted in Fe and Ni relative to the taenite. BSE images indicate that this weathering product is free of Fe,Ni inclusions, but its mineralogy cannot be determined solely from the EPMA data. To the authors' knowledge no hydrous Fe-Ni-Mg silicates have been recorded, although a number of hydrous Ni-Mg and Ni-silicates are known, which include nepouite $(Ni,Mg)_3Si_2O_5(OH)_4$, falcondoite $(Ni,Mg)_4Si_6O_{15}(OH)_2 \cdot 6H_2O$ and pecoraite $Ni_3Si_2O_5(OH)_4$. The latter mineral was first described from Wolf Creek, a very heavily terrestrially weathered meteorite from Western Australia, by Faust et al. (1969). This serpentine-group mineral is the Ni analog of clinochrysotile and its chemical composition is listed in Table 5. Pecoraite occurs in association with goethite, Ni-maghemite, jarosite, reevesite $(Ni_6Fe_2[OH]_{16}CO_3 \cdot 4H_2O]$ and iron and nickel phosphates in Wolf Creek (White et al., 1967). We conclude that the alteration product of taenite grains in ALHA 78045 is either a very fine-scale intergrowth of pecoraite with Fe-Mg phyllosilicates such as cronstedtite, a new Fe-Mg analog of pecoraite with the approximate formula $(Fe,Ni,Mg)_3\ Si_2O_5(OH)_4$, or a non-crystalline, gel-like weathering product, as suggested by Zolensky and Gooding (1986) for some of the weathering products in the Antarctic find ALH 77003.

5.4.4. *Implications for Chemical Weathering of Primary Meteoritic Silicates*

Regardless of the host of Si, Mg and Ca in products of weathering of 'hot' desert and Antarctic meteorites (and New Concord), the presence of these ions shows that primary silicates within the ordinary chondrites (olivine, orthopyroxene, clinopyroxene) have undergone dissolution. Given the differences in Fe/Si ratios between weathering products in meteorites from the two environments (Fig. 5), the primary silicates must be more susceptible to dissolution (relative to metal and sulphide) under Antarctic conditions.

A number of lines of evidence indicate that the limited concentrations of Si, Mg and Ca in 'hot' desert weathering

products are derived from dissolution of primary silicates by acidic pore fluids produced during oxidation and hydration of Fe,Ni metal and troilite. This evidence includes the close spatial relationship between heavily altered Fe,Ni grains and dissolution pores (Figs. 3a–3d) and enrichment of Si, Mg and Ca in the outermost (i.e., earliest-formed) parts of the weathering rim from Daraj 014 (Fig. 2). Other workers have found evidence for weathering of primary silicates in 'hot' desert environments. SIMS analyses of two Libyan Shergottites by Crozaz and Wadhwa (2001) demonstrated light REE enrichment of olivine and pyroxene, which they interpreted as indicating terrestrial weathering of those minerals; significantly they found no such enrichment in the feldspathic glass. Our EPMA data also shows that the weathering products have negligible concentrations of Al_2O_3, indicating that feldspar does not contribute significantly to the weathering reactions. It is important to note that the heavily-weathered 'hot' desert meteorites studied here contain some relatively large dissolution pores (Figs. 3a and 3c). We suggest that these large pores were predominantly formed during relatively late stages of weathering after most of the Fe-oxide/oxyhydroxides had been formed so that the Si, Mg and Ca ions could not be incorporated into those weathering products. It is likely, therefore, that ions liberated by the late-stage dissolution are lost from the meteorite and this is supported by Mössbauer spectroscopy data in Bland et al. (1998b) which shows that volumes of olivine and pyroxene in H, L and LL ordinary chondrites decrease in a very regular manner with increasing weathering.

EPMA data for the four least-weathered Antarctic meteorites (Table 4) show that the average concentration of Si and Mg in weathering products decreases with increasing oxidation. These observations suggest a similar process to the 'hot' desert meteorites whereby olivine and pyroxene grains are susceptible to dissolution during the earliest stages of weathering when their external surfaces are freshly exposed. The early-formed parts of Fe-oxide/oxyhydroxide rims thus become enriched in Si, Mg and Ca ions. With progressive weathering the surfaces of Fe,Ni metal grains retreat behind Fe-oxide/oxyhydroxides, intergranular pores are occluded by the weathering products and surfaces of olivine and pyroxene grains are coated with a protective layer of Fe-oxide/oxyhydroxides. These three processes combine to slow rates of weathering of primary silicate minerals. Buchwald and Clarke (1989) also observed that dissolution of silicates may accompany the chemical weathering of Fe,Ni metal grains in Antarctic ordinary chondrites.

5.4.5. *Mass Balance Within Antarctic Meteorites*

This work has demonstrated that primary silicate minerals readily undergo chemical weathering in Antarctic environments. One anomaly however is that the Antarctic weathering products all have high Si/Mg ratios ($Si/Mg_{cronstedtite} = \sim 18$) whereas the most abundant primary silicates in L5/6 ordinary chondrites have much lower ratios ($Si/Mg_{olivine} = 0.8$, $Si/Mg_{orthopyroxene} = 1.5$). Thus, Antarctic meteorites must have another sink for Mg ions. The most likely candidate comes from work on carbonate weathering products that have been found on the surfaces of Antarctic finds (Jull et al., 1988; Velbel, 1988; Velbel et al., 1991). These weathering products, which mainly occur as efflorescences on the outer surfaces of meteorites, including equilibrated ordinary chondrites, comprise the hydrous Mg-carbonates nesquehonite ($Mg[HCO_3][OH] \cdot 2H_2O$) and hydromagnesite ($(Mg_5[CO_3]_4[OH]_2 \cdot 4H_2O$). Evaporites that have been described in other studies include epsomite ($MgSO_4 \cdot 7H_2O$), starkeyite ($MgSO_4 \cdot 4H_2O$) and gypsum ($CaSO_4 \cdot 2H_2O$) (Marvin, 1980). Jull et al. (1988) and Velbel et al. (1991) concluded that Mg for the nesquehonite was derived from within the host meteorites and specifically from weathering of olivine, whereas oxygen, carbon and water were derived from the Antarctic atmosphere and hydrosphere. Carbon and oxygen isotope data in Jull et al. (1988) show that nesquehonite formed very recently (after A.D. 1950) using water derived from the Antarctic ice at ~0°C. A reaction to form nesquehonite from olivine is reproduced below (from Velbel et al., 1991):

$$(Fe_xMg_{1-x})_2SiO_4 + (8-5x)H_2O + (2-2x)CO_2 + 0.5xO_2 \rightarrow (2-2x)(Mg[HCO_3][OH] \cdot 2H_2O) + 2xFeOOH + H_4SiO_{4(aq)} \quad (2)$$

where x denotes the mole fraction of fayalite in the olivine. For ALHA 78045 the value of x is 0.25. The by-products of the reaction above are Fe-oxyhydroxide and silica in solution. The reaction can be rewritten so that cronstedtite is formed instead, although additional Fe is required, in this case derived from Fe,Ni metal:

$$(Fe_xMg_{1-x})_2SiO_4 + 20xFe_{0.7},Ni_{0.3} + 26xH_2O + 6xCO_2 + 6xO_2 \rightarrow 1.5[Mg(HCO_3)(OH) \cdot 2H_2O] + [Fe^{2+}{}_2Fe^{3+})[Si\,Fe^{3+}O_5](OH)_4 + 1.5NiO \quad (3)$$

Using a simpler version of Eqn. 2, Velbel et al. (1991) calculated water activities for the reactions under Antarctic conditions, which were consistent with the reactions being mediated by liquid water present as thin films (hydrocryogenic diagenesis of Gooding, 1986) or brines. The work by Jull et al. (1988) and Velbel et al. (1991) demonstrates that the evaporites formed during recent exposure of the meteorite but they are unclear whether all of the reactions above took place in such a short space of time.

5.4.6. *Microtextural Controls on Alteration of Fe,Ni Metal*

Most Fe,Ni metal grains progressively weather by a front of alteration products moving steadily from the outer surface towards the inside of the grain, eventually leaving a concentrically laminated pseudormorph. However, a number of Fe,Ni metal grains had an exsolution microtexture that affected the passage of the weathering front. Some grains in ALH 78112 internal were composed of a relatively coarse intergrowth of Ni-rich metal (tetrataenite) with Ni-poor metal (?kamacite) and the Ni-poor metal was more susceptible to alteration, leaving a denticulated outer margin to the remaining Fe,Ni metal (Fig. 8d). Alteration textures in ALH 78045 were somewhat different and comprised a fine-scale lamellar intergrowth of two minerals, probably kamacite and taenite. As with ALH 78112, one of the minerals in the intergrowth is more susceptible to chemical weathering and so remains as inclusions within weathering products in partially weathered parts of the grains (Figs. 11a

and 11b). This microtexture is comparable to 'black plessite' where the kamacite and taenite have a specific orientation relationship, $\{111\}_{taenite} \parallel \{011\}_{kamacite}$. These microstructures are very common within the taenite regions of the Widmanstätten pattern of iron meteorites (Zhang et al., 1993), but have also been described from within the zoned taenite portion of a Widmanstätten texture developed in metal veins from the H6 ordinary chondrite Portales Valley (Sepp et al., 2001). Within this meteorite the microtexture comprises 20 to 100 nm wide taenite rods in a kamacite matrix. The relatively small size of the taenite rods shows that the microtexture had formed by the decomposition of martensite (α_2-iron) at low-T (possibly $<$ 100°C) and at a slow cooling rate.

5.5. Carbonate, Sulphate and Silica Weathering Products

The mineralogical variety of weathering products is much greater in 'hot' desert than Antarctic meteorites and includes barite, gypsum, jarosite, Ca-carbonate and silica. A number of other workers have described barite, gypsum and Ca-carbonate from 'hot' desert finds (e.g., Stelzner et al., 1999; Crozaz and Wadhwa, 2001). The barium for barite is probably atmospherically-derived because it is a common constituent of desert varnish, which can coat the surfaces of 'hot' desert meteorites (Lee and Bland, 2003). Barrat et al. (1999) have demonstrated that 'hot' desert carbonates can form rapidly ($<$63 yr of terrestrial exposure), similar to the timescale of carbonate formation in Antarctic meteorite weathering (Jull et al., 1988; Velbel et al., 1991). Silica is uncommon in 'hot' desert finds and may be the equivalent to silica glazes that occur on a variety of rock types in 'hot' deserts. White et al. (1967) described cavity-filling opal from the highly weathered Australian iron meteorite Wolf Creek, which probably has a similar origin.

6. IMPLICATIONS

6.1. Impact of Terrestrial Weathering on the Physical Properties of Meteorites

To quantify the physical impact of terrestrial weathering on meteorites, especially occlusion of porosity and brecciation, we have calculated the changes in volume resulting from the alteration of primary minerals to a range of weathering products. We have adopted the approach described by Velbel (1993), which is based on the Pilling-Bedworth rule that is used by metallurgists to determine the nature of oxide layers on metals. This rule states that the volume of reactant produced by weathering of a given volume of a precursor mineral can be calculated by assuming that one element, for example Fe or Si, is conserved. All that is required for these calculations are data on the stoichiometric coefficients and molar volumes of precursors and reactants and values for the minerals of interest in this study are listed in Table 6. Using these data the volume of product mineral formed per unit volume of reactant (V_p/V_r) can be calculated from Eqn. 4 below:

$$\frac{V_p}{V_r} = \frac{ne_r\, V_p^0}{ne_p\, V_r^0} \quad (4)$$

where n_e = stoichiometric coefficient of element e (Fe or Si) in the reactant (r) or product (p) and V^0 = molar volume of the reactant (r) or product (p). If $V_p/V_r > 1$ the volume of the product will be greater than the volume of reactant whereas if $V_p/V_r < 1$ the opposite will be true. Results of calculations for the most common reactant and product minerals found in this study are listed in Table 7. These data show that alteration of kamacite and taenite to all Fe-oxide/oxyhydroxide weathering products will result in a net volume increase, but the volume increase is significantly smaller for weathering of troilite (Table 7). By contrast, weathering of olivine and orthopyroxene to Fe-oxide/oxyhydroxides leads to a significant reduction in volume (assuming Si is lost from the meteorite). If Si is conserved instead of Fe to make cronstedtite, the weathering reaction yields a significant increase in volume (Table 7). It must be emphasised that these calculations assume that the weathering products have no inter or intracrystalline porosity. TEM observations show that most Fe-oxides and hydroxides have a low porosity (Fig. 3d), although porosity may be significant in volumes of phyllosilicates (Fig. 11a). The effect of porosity within alteration products on the calculations is discussed below.

Table 6. The stoichiometric coefficients and molar volumes of the main minerals of interest in weathered L5/L6 ordinary chondrites.

Mineral, formula	Stoichiometric coefficient (n_e)	Molar volume (V^0, cm^3)
Akaganéite, β-$Fe^{3+}OOH$	1_{Fe}	25.147[a]
Cronstedtite, $(Fe_{2.2}^{2+}\ Fe_{0.8}^{3+})$ $(Si_{1.2}\ Fe_{0.78}^{3+}\ Al_{0.02})O_5(OH)_4$	3.8_{Fe}, 1.2_{Si}	112.621[b]
Goethite, α-$Fe^{3+}OOH$	1_{Fe}	20.693[c]
Hibbingite, γ-$Fe_2^{2+}(OH)_3Cl$	2_{Fe}	62.057[d]
Kamacite, α-$Fe_{0.9}^{0},Ni_{0.1}$	0.9_{Fe}	7.101[a]
Lepidocrocite, γ-$Fe^{3+}OOH$	1_{Fe}	22.492[c]
Maghemite, γ-$Fe_2^{3+}O_3$	2_{Fe}	29.114[a]
Olivine, $Mg_{1.5}Fe_{0.5}^{2+}SiO_4$	0.5_{Fe}, 1_{Si}	43.623[a,e]
Orthopyroxene, $Mg_{1.5}Fe_{0.5}^{2+}Si_2O_6$	0.5_{Fe}, 2_{Si}	62.671[a,f]
Taenite, β-$Fe_{0.7}^{0},Ni_{0.3}$	0.7_{Fe}	6.931[a]
Troilite, $Fe^{2+}S$	1_{Fe}	17.905[a]

[a] Calculated from unit cell parameters using data in Deer et al. (1992). [b] From data for the Herja sample of cronstedtite described in Hybler et al. (2000). [c] Data from Velbel (1993, Table 1). [d] Using data in Saini-Eidukat et al. (1994). [e] Using unit-cell parameters for forsterite. [f] Using unit-cell parameters for orthorhombic enstatite.

Data in the upper part of Table 7 can be used to determine the mean change in volume of each reactant mineral as it is altered to yield a given suite of weathering products (mV_p/mV_r). We have assumed four different scenarios based on different weathering environments. In the 'hot' desert environment we have assumed that kamacite, taenite and troilite weather to goethite, lepidocrocite and maghemite in equal proportions. In the first Antarctic case (Antarctic-1) we have assumed that kamacite and taenite weather to all of the listed Fe-oxides and oxyhydroxides in equal proportions. In the second Antarctic case (Antarctic-2) we have assumed that kamacite and taenite weather to all Fe-oxides and oxyhydroxides in equal proportions and olivine and orthopyroxene weather to cronstedtite only, with Fe being conserved. In the final case (Antarctic-3) we assume the same reactions as Antarctic-2, but that Si rather than Fe is conserved to form cronstedtite. Using data at the foot of Table 7 it is straightforward to calculate the

Table 7. Changes in volume resulting from weathering of the main primary minerals in L5/L6 ordinary chondrites to a variety of alteration products, assuming that Fe is conserved.

Product minerals	*Reactant minerals*				
	Kamacite	Taenite	Troilite	Olivine	Orthopyroxene
			(V_p/V_r)		
Akaganéite	3.19	2.54	1.40	0.29	0.20
Cronstedtite	3.76	2.99	1.66	0.34 (2.15)[a]	0.24 (3.00)[a]
Goethite	2.62	2.09	1.16	0.24	0.17
Hibbingite	3.93	3.13	1.73	0.36	0.25
Lepidocrocite	2.85	2.27	1.26	0.24	0.18
Maghemite	1.85	1.47	0.81	0.17	0.12
			(mV_p/mV_r)		
Hot desert	2.44	1.94	1.08	—	—
Antarctic-1	3.03	2.42	—	—	—
Antarctic-2	3.03	2.42	—	0.34 (0.43)[b]	0.24 (0.30)[b]
Antarctic-3	3.03	2.42	—	2.15 (2.69)[b]	3.00 (3.75)[b]

[a] Figures in parenthesis are calculated by assuming that Si is conserved. [b] Figures in parentheses give the change in volume if the cronstedtite weathering products have a 25% porosity.

overall change in volume of an ordinary chondrite during progressive weathering in different environments (Table 8). For these calculations we have used the average mineralogy of L class ordinary chondrites in McSween et al. (1991) and additionally assumed that when it falls to Earth the average L-class ordinary chondrite has a 10% porosity (Table 8, column 1). The change in volume (cV) upon weathering of mineral i was calculated using the following equation:

$$cV = \left[\left(\frac{V_i}{100} \times (100-W)\right) + \left(\left(\frac{V_i}{100} \times W\right) \times \left(\frac{mV_p}{mV_r}\right)\right)\right] \quad (5)$$

where V_i = volume of mineral i in 1 cm^3 of meteorite, W = degree of weathering (%) of the meteorite overall, assuming that all reactive components weather at an equal rate, and mV_p/mV_r is the mean volume of product mineral produced per unit volume of reactant.

Results from a specimen calculation for 20% weathering are given in Table 8 (columns 7–10) and results for 0 to 60% weathering are plotted in Figure 13. This graph shows that in the 'hot' desert and Antarctic-1 scenarios terrestrial weathering results in a considerable increase in the solid volume of the meteorite; the degree of volume increase is slightly greater in the Antarctic-1 environment as troilite does not weather (Fig. 13). These data show that a 10% initial porosity can easily accommodate the extra volume of weathering products formed in the hot desert and Antarctic-1 models. Although we have observed brecciation produced by dilation of intergranular fractures, mainly in 'hot' desert meteorites, our calculations show that expansion is not necessary to accommodate the weathering products unless the meteorite has an unusually large volume of Fe,Ni metal and/or a prefall porosity of significantly $<$ 10%. White et al. (1967) noted that although the Wolf Creek iron meteorite had been virtually reduced to a goethite-maghemite pseudomorph by intense terrestrial weathering, the meteorite pieces had not disintegrated. They concluded that "The great expansion accompanying oxidation has apparently been accommodated without disrupting the specimens." Results for the Antarctic-2 and Antarctic-3 cases show that cronstedtite formation from weathering of olivine and orthopyroxene has a

Table 8. Calculated change in volume resulting from weathering of 1 cm^3 of ordinary chondrite with 10% initial porosity.

		Mean volume change on weathering of each mineral (mV_p/mV_r)				Volume of remaining mineral plus reaction product after 20% weathering (cm^3)			
	Initial volume (V_i cm^3)[a]	Hot desert	Antarctic-1	Antarctic-2	Antarctic-3	Hot desert	Antarctic-1	Antarctic-2	Antarctic-3
Olivine	0.410	—	—	0.34	2.15	0.410	0.410	0.356	0.504
Orthopyroxene	0.222	—	—	0.24	3.00	0.220	0.222	0.188	0.311
Kamacite[b]	0.033	2.44	3.03	3.03	3.03	0.042	0.046	0.046	0.046
Taenite[b]	0.033	1.94	2.42	2.42	2.42	0.039	0.042	0.042	0.042
Troilite	0.036	1.08	—	—	—	0.037	0.036	0.036	0.036
Others	0.166	—	—	—	—	0.167	0.167	0.166	0.166
Solid volume	0.900					0.916	0.923	0.834	1.105
Porosity	0.100					0.084	0.077	0.166	0[c]

[a] Volumetric abundances were determined by dividing wt.% abundance from McSween et al. (1991) by density of each mineral. [b] Assumes a kamacite/taenite ratio (wt) of 1.6. [c] All porosity has been filled and the meteorite must increase in overall volume to accommodate the weathering products.

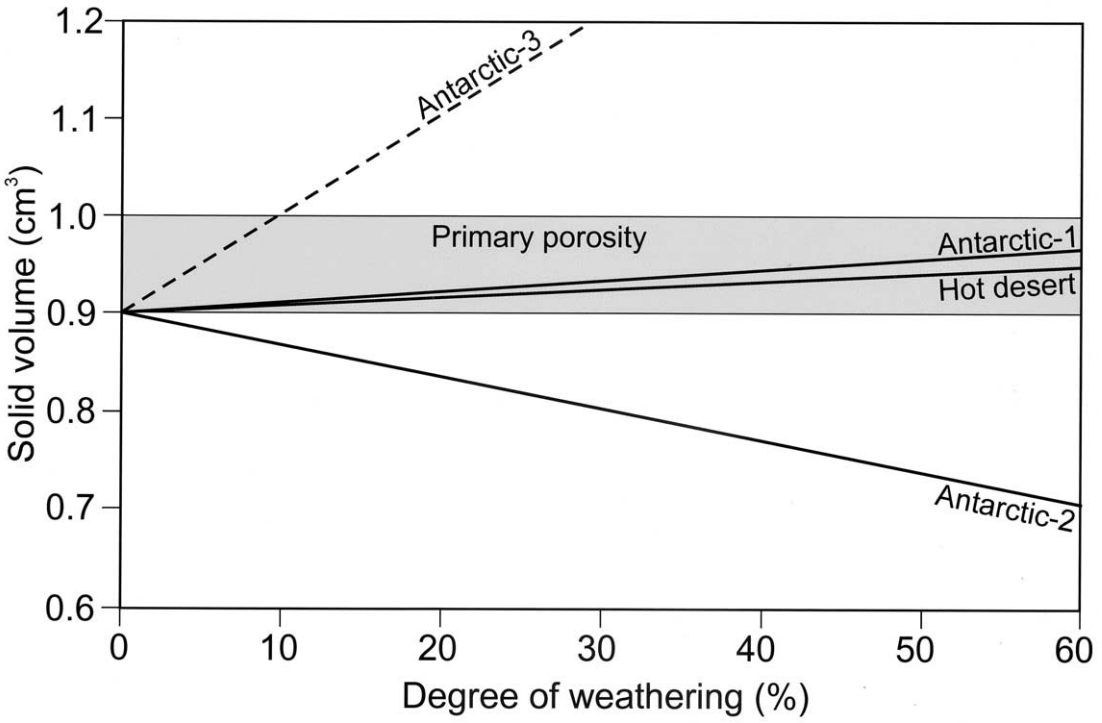

Fig. 13. Graph illustrating results of four models of how the solid volume of 1 cm^3 of a L5/6 ordinary chondrite with 10% initial porosity may change during terrestrial weathering. Note that weathering in the hot desert and Antarctic-1 scenarios leads to a small increase in solid volume, which can be accommodated by occlusion of primary porosity, whereas the Antarctic-2 scenario leads to a dramatic reduction in solid volume of the meteorite, creating new (secondary) porosity. The Antarctic-3 scenario, which yields an equally dramatic increase in solid volume, is illustrated for comparison but is unrealistic because the volume of cronstedtite formed in Si-conservative reactions is limited by the relatively small volume of Fe,Ni metal available. In addition, the meteorite should start to fragment once the solid volume exceeds 1 cm^3.

very significant impact on changes in volume of the meteorite. If olivine and orthopyroxene alter to cronstedtite with Fe conserved (Antarctic-2), the solid volume of the meteorite decreases dramatically (Fig. 13). Assuming the cronstedtite has 25% intercrystalline porosity makes very little difference to this result (Table 7). The porosity decrease upon alteration may explain why very little brecciation was recorded within Antarctic finds. In addition it may account for the unexpected findings by Consolmagno et al. (1998) that the porosity of Antarctic ordinary chondrites ranges from 0 to 20% and can be greater than the porosity of some ordinary chondrite falls. We suggest that this increase in porosity during weathering is likely to be much more pronounced for varieties of Antarctic meteorites that lack Fe,Ni metal. However, if olivine and orthopyroxene alter to cronstedtite with Si conserved (Antarctic-3 case), the volume of the meteorite increases dramatically, even more so if the cronstedtite has a significant intercrystalline porosity (Table 7). It must be recognised that the Antarctic-3 case is an oversimplification because cronstedtite requires large quantities of Fe^{2+} and Fe^{3+}, which can only be derived from Fe,Ni metal altering within the meteorite (as expressed in Eqn. 3). As far less Fe,Ni metal than olivine and orthopyroxene is initially present within the meteorite, the volume of cronstedtite that can be formed in Si-conservative reactions is limited. Note also that in the Antarctic-3 case the meteorite will begin to disintegrate after ~10% of weathering and all available porosity has been occluded.

6.2. Using Weathered Meteorites to Understand Parent Body Aqueous Alteration

Results of this work have both positive and negative implications for the use of meteorite finds to study low temperature aqueous alteration within the regoliths of asteroidal and planetary parent bodies. On the positive side, we have shown that cronstedtite is commonplace in highly weathered Antarctic ordinary chondrites. This mineral is also abundant in the matrices of CM2 carbonaceous chondrites (e.g., Müller et al., 1979; Barber 1981, 1985) and is inferred to have been the first phyllosilicate to have formed during aqueous alteration within the regoliths of their asteroidal parent bodies (e.g., Tomeoka and Buseck, 1985; Zolensky et al., 1993; Browning et al., 1996). Thus, there may be many similarities between the chemical microenvironments within ordinary chondrites undergoing weathering on or within the Antarctic ice at the present day (e.g., temperature, pH and water/rock ratios) and conditions within carbonaceous chondrite parent bodies ~4.4 Ga ago. There are also obvious differences, in particular the much coarser grain size of ordinary chondrites and exposure to the terrestrial atmosphere, which promotes formation of weathering products rich in Fe^{3+}. However, more detailed analysis of weathering products in Antarctic ordinary chondrites may provide new insights into conditions of aqueous alteration within asteroids, as initially proposed by Zolensky and Gooding (1986).

The negative implications of this work are that we have demonstrated that considerable volumes of hydrous silicate minerals can readily form during terrestrial weathering of meteorite finds, in both 'hot' desert and Antarctic environments. Thus, care must be exercised when interpreting clays and phyllosilicates in meteorite finds from both asteroidal parent bodies and planetary regoliths (e.g., Martian meteorites, Sautter et al., 2002) as products of preterrestrial aqueous alteration. As described above, cronstedtite can form by both terrestrial and preterrestrial aqueous alteration and it is likely that smectite can also form in both environments. This work has also shown that very significant weathering of Fe,Ni metal can take place within ordinary chondrite falls during curation under museum conditions. By analogy with the weathered meteorite finds, clays and phyllosilicates are also likely to form during museum weathering of falls.

7. CONCLUSIONS

Results of this study have demonstrated that equilibrated ordinary chondrites recovered from 'hot' deserts and Antarctica contain a variety of terrestrial weathering products that include rare Fe-chlorides and possibly previously unknown Fe,Ni-oxyhydroxides and Fe,Mg(Ni) phyllosilicates. New Concord, a 143-yr-old fall, also contains significant volumes of terrestrial weathering products. Antarctic meteorites differ from 'hot' desert finds in the chemical composition and mineralogy of Fe-oxides and oxyhydroxides (Cl-bearing minerals are more common) and much greater abundance of silicate mineral weathering products. The abundance of Cl-bearing weathering products is probably due to sources of Cl in Antarctica, but the silicate minerals are more difficult to account for. We suggest that terrestrially formed clays and phyllosilicates are likely to be ubiquitous in meteorite finds but few have been previously described because most work on terrestrially weathered meteorites has not applied the high-resolution imaging and analysis techniques that are routinely used for studying meteorite falls. Thus, great care must be taken when using data from 'hot' desert and Antarctic meteorites from primitive asteroidal and planetary parent bodies to investigate low temperature aqueous alteration within the regoliths of their parent bodies. The potential formation of clays and phyllosilicates in addition to Fe-oxide/oxyhydroxides during museum curation is of particular concern and is currently being investigated.

Acknowledgments—We thank John Gileece for making the thin sections and Robert MacDonald for assistance with the SEM and electron probe. We are also grateful to Professor Alan Craven (Physics and Astronomy, Glasgow) for access to TEM and Ar ion milling facilities and Colin How and Brian Miller respectively for assistance with those instruments. We thank ANSMET for provision of the Antarctic meteorite samples used in this study, the Western Australian Museum for the specimens of Billygoat Donga and Forrest 009, EUROMET (Milton Keynes) for the loan of samples from the Algerian and Lybian Sahara and the Natural History Museum (London) for the loan of Barwell and New Concord. This work was funded by NERC grant NER/B/S/2000/00343 and the Royal Society. Lastly, we thank Alex Bevan, Mike Velbel and Mike Zolensky for very thorough, and sometimes witty, reviews that have considerably improved this manuscript.

Associate editor: M. M. Grady

REFERENCES

Ash R. D. and Pillinger C. T. (1995) Carbon, nitrogen and hydrogen in Saharan chondrites: The importance of weathering. *Meteorit. Planet. Sci.* **30,** 85–92.

Barber D. J. (1981) Matrix phyllosilicates and associated minerals in C2M carbonaceous chondrites. *Geochim. Cosmochim. Acta* **45,** 945–970.

Barber D. J. (1985) Phyllosilicates and other layer structured materials in meteorites. *Clay Miner.* **20,** 415–454.

Barrat J. A., Gillet P., Lècuyer C., Sheppard S. M. F., and Lesourd M. (1999) Formation of carbonates in the Tatahouine meteorite. *Science* **280,** 412–414.

Benoit P. H. and Sears D. W. G. (1999) Accumulation mechanisms and the weathering of Antarctic equilibrated ordinary chondrites. *J. Geophys. Res.* **104,** 14159–14168.

Bland P. A., Kelley S. P., Berry F. J., Cadogan J. M., and Pillinger C. T. (1997) Artificial weathering of the ordinary chondrite Allegan: Implications for the presence of Cl- as a structural component of akaganéite. *Am. Mineral.* **82,** 1187–1197.

Bland P. A., Berry F. J., and Pillinger C. T. (1998a) Rapid weathering in Holbrook: An iron-57 Mössbauer spectroscopy study. *Meteorit. Planet. Sci.* **33,** 127–129.

Bland P. A., Sexton A. S., Jull A. J. T., Bevan A. W. R., Berry F. J., Thornley D. M., Astin T. R., Britt D. T., and Pillinger C. T. (1998b) Climate and rock weathering: A study of terrestrial age dated ordinary chondritic meteorites from hot desert regions. *Geochim. Cosmochim. Acta* **62,** 3169–3184.

Bland P. A., Jull A. J. T., and Bevan A. W. R. (2000a) Ancient meteorite finds and the Earth surface environment. *Quat. Res.* **53,** 131–142.

Bland P. A., Lee M. R., Sexton A. S., Franchi I. A., Fallick A. E. T., Miller M. F., Cadogan J. M., Berry F. J., and Pillinger C. T. (2000b) Aqueous alteration without a pronounced oxygen isotope shift: Implications for asteroidal processing of chondritic materials. *Meteorit. Planet. Sci.* **35,** 1387–1395.

Boyd T. and Scott S. D. (1999) Two-XRD-line ferrihydrite and Fe-Si-Mn oxyhydroxide mineralization from Franklin Seamount, western Woodlark Basin, Papua New Guinea. *Can. Mineral.* **37,** 973–990.

Browning L. B., McSween H. Y., and Zolensky M. E. (1996) Correlated alteration effects in CM carbonaceous chondrites. *Geochim. Cosmochim. Acta* **60,** 2621–2633.

Buchwald V. F. and Clarke R. S., Jr.. (1995) Corrosion of Fe-Ni alloys by Cl-containing akaganéite (β-FeOOH): The Antarctic meteorite case. *Am. Mineral.* **74,** 656–667.

Buchwald V. F. and Koch C. B. (1995) Hibbingite (β-$Fe^{2+}{}_2(OH)_3Cl$), a chlorine-rich corrosion product in meteorites and ancient iron objects. *Meteorit. Planet. Sci.* **30,** A493.

Cassidy W., Harvey R., Schutt J., Delilse G., and Yanai K. (1992) The meteorite collection sites of Antarctica. *Meteoritics* **27,** 490–525.

Crozaz G. and Wadhwa M. (2001) The terrestrial alteration of Saharan Shergottites Dar el Gani 476 and 489: A case study of weathering in a hot desert environment. *Geochim. Cosmochim. Acta* **65,** 971–978.

Consolmagno G. J. and Britt D. T. (1998) The density and porosity of meteorites from the Vatican collection. *Meteorit. Planet. Sci.* **33,** 1231–1241.

Consolmagno G. J., Britt D. T., and Stoll C. P. (1998) The porosities of ordinary chondrites: Models and interpretations. *Meteorit. Planet. Sci.* **33,** 1221–1229.

Consolmagno G. J., Bland P. A., and Strait M. M. (1999) A preliminary scanning electron microscopy study of microcrack porosity in meteorites. *Meteorit. Planet. Sci.* **34,** A28–A29.

Corrigan C. M., Zolensky M. E., Dahl J., Long M., Weir J., Sapp C., and Burkett P. J. (1997) The porosity and permeability of chondritic meteorites and interplanetary dust particles. *Meteorit. Planet. Sci.* **32,** 509–515.

Deer W. A., Howie R. A., and Zussman J. (1992) *An introduction to the rock-forming minerals*. Longman, Harlow, UK.

Faust G. T., Fahey J. T., Mason B., and Dwornik E. J. (1969) Pecoraite, $Ni_6Si_4O_{10}(OH)_8$, nickel analog of clinochrysotile, formed in the Wolf Creek meteorite. *Science* **165,** 59–60.

Flynn G. J., Moore L. B., and Klöck W. (1999) Density and porosity of stone meteorites: Implications for the density, porosity, cratering, and collisional disruption of asteroids. *Icarus* **142,** 97–105.

Goede A., Atkinson T. C., and Rowe P. J. (1992) A giant Late Pleistocene halite speleothem from Webbs cave, Nullarbor Plain, southeastern Australia. *Helectite* **30,** 3–7.

Gooding J. L. (1986) Clay-mineraloid weathering products in Antarctic meteorites. *Geochim. Cosmochim. Acta* **50,** 2215–2223.

Graham A. L. (1989) The Meteoritical Bulletin. *Meteoritics* **24,** 57–60.

Graham A. L. (1990) The Metoritical Bulletin. *Meteoritics* **25,** 59–70.

Grossman J. N. (1994) The Meteoritical Bulletin, No. 76, 1994 January: The US Antarctic meteorite collection. *Meteoritics* **29,** 100–143.

Harvey R. P. and Score R. (1991) Direct evidence of in-ice of pre-ice weathering of Antarctic meteorites. *Meteoritics* **26,** 343–344.

Herbert R. B. (1999) Compositional zoning in Fe oxyhydroxides: An electron microprobe study. *GFF* **121,** 221–226.

Hochella M. F., Jr., Moore J. N., Golle U., and Putnis A. (1999) A TEM study of samples from acid mine drainage systems: Metal-mineral association with implications for transport. *Geochim. Cosmochim. Acta* **63,** 3395–3406.

Hutchison R., Alexander C. M. O., and Barber D. J. (1987) The Semarkona meteorite: First recorded occurrence of smectite in an ordinary chondrite, and its implications. *Geochim. Cosmochim. Acta* **51,** 1875–1882.

Hybler J., Petrícek V., Durovic S., and Smrcok L. (2000) Refinement of the crystal structure of cronstedtite-1T. *Clays Clay Miner.* **48,** 331–338.

Ikeda Y, Kojima H (1991) Terrestrial alteration of Fe-Ni metals in Antarctic ordinary chondrites and the relationship to their terrestrial ages. In *Proceedings of the NIPR Symposium on Antarctic Meteorites* **4,** 307–318.

Jull A. J. T., Cheng S., Gooding J. L., and Velbel M. A. (1988) Rapid growth of magnesium-carbonate weathering products in a stony meteorite from Antarctica. *Science* **242,** 417–419.

Langenauer M. and Krähenbühl U. (1993) Halogen contamination in Antarctic H5 and H6 chondrites and relation to sites of recovery. *Earth Planet. Sci. Lett.* **120,** 431–442.

Lee M. R. and Bland P. A. (2003) Dating climatic change in hot deserts using desert varnish on meteorite finds. *Earth Planet. Sci. Lett.* **206,** 187–198.

Lee M. R., Bland P. A., and Graham G. (2003) Preparation of TEM samples by focused ion beam (FIB) techniques: Applications to the study of clays and phyllosilicates in meteorites. *Mineral. Mag.* **67,** 581–592.

Marvin U. B. (1980) Magnesium carbonate and magnesium sulphate deposits on Antarctic meteorites. *Antarctica J. U. S.* **15,** 54–55.

McSween H. Y., Bennett M. E., III, and Jarosewich E. (1991) The mineralogy of ordinary chondrites and implications for asteroid spectrophotometry. *Icarus* **90,** 107–116.

Müller W. F., Kurat G., and Kracher A. (1979) A chemical and crystallographic study of cronstedtite in the matrix of the Cochabamba (CM2) carbonaceous chondrite. *Tsherm. Mineral. Petrogr. Mitteil.* **26,** 293–304.

Newman A. C. D, Brown G (1987) The chemical constitution of clays. In *Chemistry of Clays and Clay Minerals* (ed. A. D. C. Newman), *Mineral. Soc. Monogr.* **6**, 1–128.

Nishiizumi K., Murrell M. T., Arnold J. R., Elmore D., Ferraro R. D., Gove H. E., and Finkel R. C. (1981) Cosmic ray produced ^{36}Cl and ^{53}Mn in Allan Hills-77 meteorites. *Earth Planet. Sci. Lett.* **52,** 31–38.

Nishiizumi K., Arnold J. R., Elmore D., Ma X., Newman D., and Gove H. E. (1983) ^{36}Cl and ^{53}Mn in Antarctic meteorites and ^{10}Be-^{36}Cl dating of Antarctic ice. *Earth Planet. Sci. Lett.* **62,** 407–417.

Nishiizumi K., Elmore D., and Kubik P. W. (1989) Update on terrestrial ages of Antarctic meteorites. *Earth Planet. Sci. Lett.* **93,** 299–313.

Rubin A. E. (1997) Mineralogy of meteorite groups. *Meteorit. Planet. Sci.* **32,** 231–247.

Rubin A. E., Zolensky M. E., and Bodnar R. J. (2002) The halite-bearing Zag and Monahans (1998) meteorite breccias: Shock metamorphism, thermal metamorphism and aqueous alteration on the H-chondrite parent body. *Meteorit. Planet. Sci.* **37,** 125–141.

Ruzicka A. (1995) Nullarbor 018: A new L6 chondrite from Australia. *Meteoritics* **30,** 102–105.

Saini-Eidukat B., Kucha H., and Keppler H. (1994) Hibbingite, γ-$Fe_2(OH)_3Cl$, a new mineral from the Duluth Complex, Minnesota, with implications for the oxidation of Fe-bearing compounds and the transport of metals. *Am. Mineral.* **79,** 555–561.

Sautter V., Barrat J. A., Jambon A., Lorand J. P., Gillet P., Javoy M., Joron J. L., and Lesourd M. (2002) A new Martian meteorite from Morocco: The nakhlite North West Africa 817. *Earth Planet. Sci. Lett.* **195,** 223–238.

Schultz L. (1986) Allende in Antarctica: Temperatures in Antarctic meteorites. *Meteoritics* **21,** 505.

Schultz L. (1990) Terrestrial ages and weathering of Antarctic meteorites. *LPI Tech. Rep.* **90-03,** 56–59.

Sepp B., Bischoff A., and Bosbach D. (2001) Low-temperature phase decomposition in iron-nickel metal of the Portales Valley meteorite. *Meteorit. Planet. Sci.* **36,** 587–595.

Shinonaga T., Endo K., Ebihara M., Heumann K. G., and Nakahara H. (1994) Weathering of Antarctic meteorites investigated from contents of Fe^{3+}, chlorine and iodine. *Geochim. Cosmochim. Acta* **58,** 3735–3740.

Stelzner T. and Hiede K. (1996) The study of weathering products of meteorites by means of evolved gas analysis. *Meteorit. Planet. Sci.* **31,** 249–254.

Stelzner T., Hiede K., Bischoff A., Weber D., Scherer P., Schultz L., Happel M., Schron W., Neupert U., Michel R., Clayton R. N., Mayeda T. K., Bonani G., Haidas I., Ivy-Ochs S., and Suter M. (1999) An interdisciplinary study of weathering effects in ordinary chondrites from the Acfer region, Algeria. *Meteorit. Planet. Sci.* **34,** 787–794.

Tomeoka K. and Buseck P. R. (1985) Indicators of aqueous alteration in CM carbonaceous chondrites: Microtextures of a layered mineral containing Fe, S, O and Ni. *Geochim. Cosmochim. Acta* **49,** 2149–2163.

Velbel M. A. (1988) The distribution and significance of evaporitic weathering products on Antarctic meteorites. *Meteoritics* **23,** 151–159.

Velbel M. A. (1993) Formation of protective surface layers during silicate-mineral weathering under well-leached, oxidizing conditions. *Am. Mineral.* **78,** 405–414.

Velbel M. A., Long D. T., and Gooding J. L. (1991) Terrestrial weathering of Antarctic stone meteorites: Formation of Mg-carbonates on ordinary chondrites. *Geochim. Cosmochim. Acta* **55,** 67–76.

White J. S., Jr., Henderson E. P., and Mason B. (1967) Secondary minerals produced by weathering of the Wolf Creek meteorite. *Am. Mineral* **52,** 1190–1197.

Wlotzka F. (1990) The Meteoritical Bulletin. *Meteoritics* **25,** 237–239.

Wlotzka F. (1993a) The Meteoritical Bulletin, Number 74, 1993 March. *Meteoritics* **28,** 146–153.

Wlotzka F. (1993b) The Meteoritical Bulletin, No. 75, 1993 December. *Meteoritics* **28,** 692–703.

Zhang J., Williams D. B., and Goldstein J. I. (1993) The microstructure and formation of duplex and black plessite in iron meteorites. *Geochim. Cosmochim. Acta* **57,** 3725–3735.

Zolensky M. E. and Gooding J. L. (1986) Aqueous alteration on carbonaceous chondrite parent bodies as inferred from weathering of meteorites in Antarctica. *Meteoritics* **21,** 548–549.

Zolensky M., Barrett R., and Browning L. (1993) Mineralogy and composition of matrix and chondrule rims in carbonaceous chondrites. *Geochim. Cosmochim. Acta* **57,** 3123–3148.